SIGNAL PROCESSING TECHNIQUES FOR NONLINEARITY IDENTIFICATION OF STRUCTURES USING TRANSIENT RESPONSE

A Thesis

presented to

the Faculty of the Graduate School

at the University of Missouri

In Partial Fulfillment

of the Requirements for the Degree

Master of Science

by

JOSEPH EUGENE DINARDO

Dr. Frank Feng, Thesis Supervisor

DECEMBER 2009

The undersigned, appointed by the dean of the Graduate School, have examined the thesis entitled

SIGNAL PROCESSING TECHNIQUES FOR NONLINEARITY IDENTIFICATION OF STRUCTURES USING TRANSIENT RESPONSE

presented by Joseph Eugene Dinardo,

a candidate for the degree of Master of Science,

and hereby certify that, in their opinion, it is worthy of acceptance.

Dr. Frank Feng

_____

Dr. P. Frank Pai

_____

Dr. Stephen Montgomery-Smith

_____

ACKNOWLEDGEMENTS

I would foremost like to thank my advisor Dr. Frank Feng for his advice and encouragement. I have learned a great deal through many discussions with him and without his wisdom this project would not have been complete. I would like to also thank the other members of the thesis committee, Dr. Frank Pai and Dr. Stephen Montgomery-Smith, for taking time out of their busy schedules for review of this work.

I would like to acknowledge Dr. Pai, who has been of tremendous help in regards to experimental setup, vibration analysis, and signal tracking. The University of Missouri has provided an optimal setting for my continued education and would like to acknowledge its assistance. I would also like to extend a gracious thank you to Dr. John Miles and the NASA-Missouri Space Grant Consortium for research funding throughout the past two and a half years. This has allowed me the opportunity to continue my education, which has undoubtedly shaped my future in a positive direction.

Undeniably, none of this work nor any previous would be possible if not for the unconditional love and support from my family. I thank my parents and sister for the guidance they have provided and the sacrifices they have made on my behalf. I also thank Sara for her continual love and encouragement. Lastly, I thank God for without him nothing is possible.

Table of Contents

List of Figures

Figure **Page**

List of Tables

Table **Page**

SIGNAL PROCESSING TECHNIQUES FOR NONLINEARITY IDENTIFICATION OF STRUCTURES USING TRANSIENT RESPONSE

Joseph Dinardo

Dr. Frank Feng, Thesis Supervisor

Abstract

In this work, an alternate method for determining nonlinearity of vibrating structures is investigated. In contrast to previous approaches, transient vibrations have been used in combination with advanced signal processing techniques to determine hardening or softening effects and strength of nonlinearity. The nonlinear characteristics of a structure can play a significant role in its behavior or response to stimuli. Thus, knowing these characteristics can lead to better design analysis and predictions of system responses.

In order to demonstrate this method's practicality and how transient vibrations can be used to determine nonlinearity, an experiment involving a cantilever beam has been subjected to vibratory analysis. The simple structure of a cantilever beam is used widely in numerous applications. In particular, Micro-Electro-Mechanical Systems (MEMS) devices known as Micromachined Vibratory Gyroscopes (MVG) make use of tuning fork type designs which utilize cantilever beams and thus can be modeled as such. In order to utilize the dynamics of MVGs to measure angular rate, their response to specific stimuli must be known. Specifically, the tuning fork tines will be subjected to

parametric excitation and Coriolis forces. An essential aspect of an MVG requires predictability. Hence, knowing the response of the system to these stimuli is crucial for design applications. MVGs require precision design and manufacturing for optimal performance.

In previous works, simulated and experimental parametric excitation of a cantilever beam has been a subject of question, as results are often contradicting. Specifically, determining whether the beam's response is characterized by a hardening or a softening effect has proven to be difficult to obtain. Moreover, theoretical response curves frequently fail to match experimental data.

Within this work, the viability of using transient vibratory analysis to determine the nonlinear characteristics of a cantilever beam has been explored. Experimental data has first been processed by using either a Butterworth 4^{th} order low pass digital filter or the empirical mode decomposition. Furthermore, a novel signal tracking technique, known as the Harmonics Tracking Method, has been used in conjunction with experimental data for signal analysis. This method was then compared to two other more traditional signal tracking techniques, the Teager-Kaiser algorithm and the Hilbert-Huang transform. Through this analysis it has been determined that a nonlinear softening effect exists within the transient response of the cantilever beam. Additionally, the effect of gravity upon the beam's response has been investigated and shown to have a slight hardening effect. It has also been determined that for transient

nonlinear analysis, the Harmonics Tracking Method used in conjunction with the empirical mode decomposition yields the best results.

Chapter 1 – Introduction

1.1 Background

This work will investigate the effects of and determination of nonlinearity within vibrating structures. Previous works of this nature have involved using steady state responses to characterize a structure's nonlinear dynamic response as either softening or hardening. Although accurate, this method requires numerous time consuming experiments which must all be precisely controlled. This leads to this type of analysis as being difficult or impossible to control in non-laboratory situations.

In contrast to this, an alternative method of collecting experimental data has been proposed which makes use of transient vibrations. This allows one to determine the nonlinear characteristics of a structure in a single and simple experiment. In addition, a novel signal tracking method, known as the Harmonics Tracking Method, has been utilized and compared to other presently used techniques for signal analysis. Also, two signal processing techniques, a low pass digital filter and the empirical mode decomposition, have been utilized and compared.

In order to illustrate the viability of this method, a cantilever beam has been subjected to vibratory analysis. More specifically, the relationship between frequency and amplitude, known as hardening or softening, has been investigated. Although simple, the cantilever beam has proven useful in numerous applications, particularly within MEMS devices.

Parametric excitation is often used to excite a MEMS structure, i.e. a cantilever beam. The response of which is then used for a given purpose. Parametric excitation

has proven to be exceptionally useful in the field of Micro-Electro-Mechanical Systems (MEMS). However, the determination of the nonlinear response of the excited cantilever beam as hardening or softening has been a subject of question. Many works have shown experimental data which contradict one another and theoretical response curves. The goal of this work is to introduce transient vibrations as a viable method for nonlinear analysis and apply it to the simple cantilever beam to determine its nonlinear characteristics as hardening or softening.

1.2 Motivation for Research

MEMS devices known as Micromachined Vibratory Gyroscopes (MVG) make use of the Coriolis force to measure either angular orientation or rotational rate. A tuning fork gyroscope is an example of a rate gyroscope which utilizes two modes of vibration to measure rotational rate [1]. Typically the tuning fork feature of the MVG is forcibly excited with axially driven vibrations. As a result of instability issues, the tuning fork tines respond with a mode one type vibration which is perpendicular to the driven excitation and opposite to one another. This driven axial excitation, known as parametric excitation, is necessary to generate this specific response of the tuning fork tines. Direct forcing will only result in the tine vibrations to coincide with one another as seen in Fig. 1.2. Once the Coriolis force acts upon the tuning fork, as a result of Coriolis acceleration, the tines will respond with flexures in a direction perpendicular to the driven mode one vibration. The combination of these two vibrations will result in a torsional vibration within the tines of the tuning fork. Using the resultant torsion, angular rate of the system can be determined.

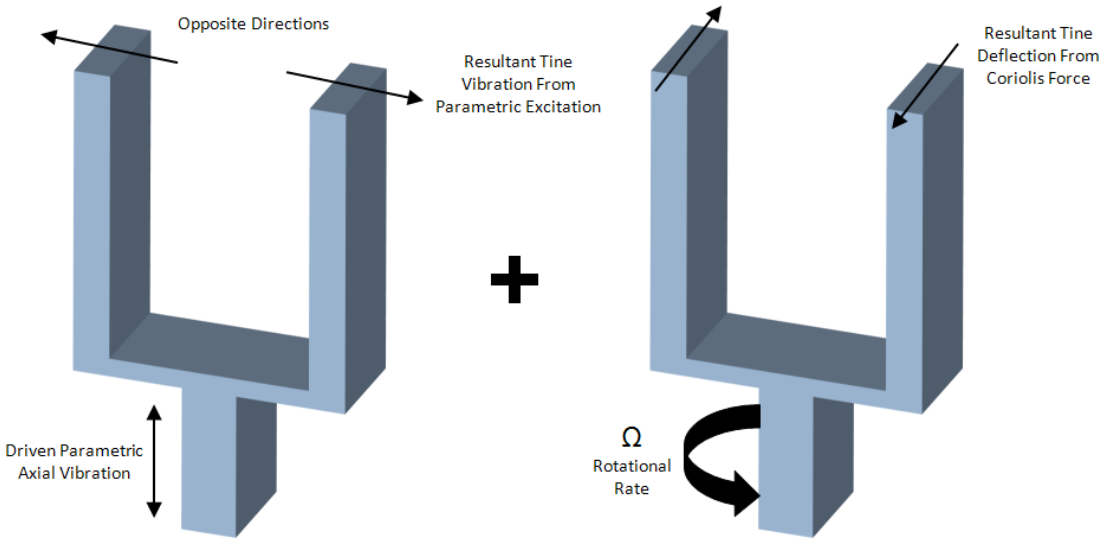

Figure 1.1. Sketch of axially driven tuning fork vibrations

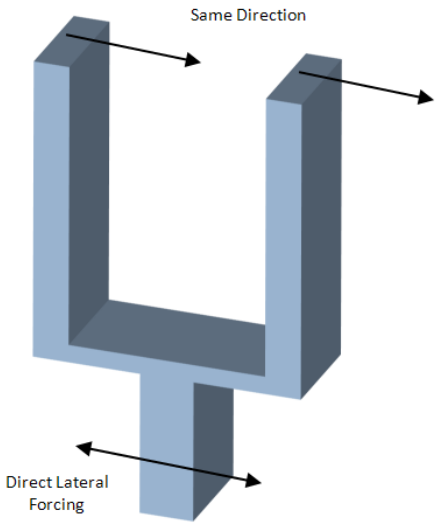

Figure 1.2 Sketch of tine vibration as a result of direct forcing

This type of MEMS device can be particularly valuable for applications involving weight and size constraints. However, currently there is a need to improve the design, performance, and robustness of MVGs [2]. Examples of various types of applications for MVGs range from defense systems such as satellites, helicopters, or micromechanical

flying insects to the entertainment sector such as video games or cellular phones. However, in order to implement MVGs, one must initially be able to accurately predict and control the driven lateral vibrations of the tuning fork tines. These tines may be modeled as cantilever beams. Understanding the response of the tuning fork design will ultimately result in a more accurate gyroscope. Determining the nonlinear response characteristics of the cantilever beam tines is imperative for design and application of the tuning fork gyroscope. It is this, which will be the center of motivation for this work as well as to introduce and prove the viability of using transient vibrations for the determination of nonlinearity.

Within the following chapters, an alternative method for nonlinear vibratory analysis will be introduced, and its viability will be tested through experiments involving a cantilever beam in various orientations and lengths. First, parametric excitation and the nonlinear characteristic which is of interest, i.e. hardening or softening, will be discussed. The conventional experimental setting and data collection method for such nonlinear analysis will be introduced and the alternative will be proposed; the results of which will then be addressed. Two signal processing methods, a Butterworth 4^{th} order low pass digital filter and the empirical mode decomposition (EMD), will then be presented and examples of their use given. Three signal tracking methods will also be briefly explained, the Teager-Kaiser algorithm (TKA), the Hilbert-Huang transform (HHT), and the harmonics tracking method (HTM). A damped nonlinear pendulum simulation will be used for validating the use of these signal tracking methods. All three of which will then be applied to the experimental data in conjunction with the two signal

processing techniques. The relationship between the instantaneous frequency and amplitude of the processed experimental data will then be explored. Next, additional signal processing considerations used with TKA will be addressed. Finally, all signal tracking results will be compared and conclusions drawn; this being followed by recommendations for future works.

Chapter 2 – Parametric Excitation and Experimental Setup

Within this chapter, parametric excitation of a cantilever beam will be discussed. As previously mentioned, MVGs often utilize this type of vibration for determination of rotational rate. In order to more accurately design and understand the dynamics of the tuning fork gyroscope, it is desired to accurately characterize its nonlinear response. Specifically, the relationship between instantaneous frequency and amplitude, which can be described as softening or hardening is of interest. Conventional experimental analysis and example results will be discussed within section 2.1. Within section 2.2, an alternative experimental set up will be introduced which promises to yield valuable data in a single and simple experiment that can be used within real world situations. Next, the raw experimental results will be examined in section 2.3.

2.1 Periodic Excitation of a Cantilever Beam

When periodic excitation is applied to a cantilever beam along the axial direction the beam's response may include significant displacement in the transversal direction. This will occur only within a specific range of excitation frequencies. Numerous works have been published which include simulation and experimentation of this phenomenon known as parametric excitation. Within these works, nonlinearities have shown to produce both softening and hardening effects upon the beam's vibration. The terms softening and hardening refer to a system's response in regards to its frequency versus amplitude relationship. Hardening indicates that as amplitude decreases, frequency will also decrease, while the term softening refers to an increase in frequency as amplitude

decreases. In addition to contradicting experimental data, previously proposed theories which attempt to predict this response curve fail to accurately portray experimental data. These theories will predict an infinitely increasing amplitude as excitation frequency increases. This, of course cannot be true. Figure 2.1 illustrates examples of theoretical, hardening, and softening response curves.

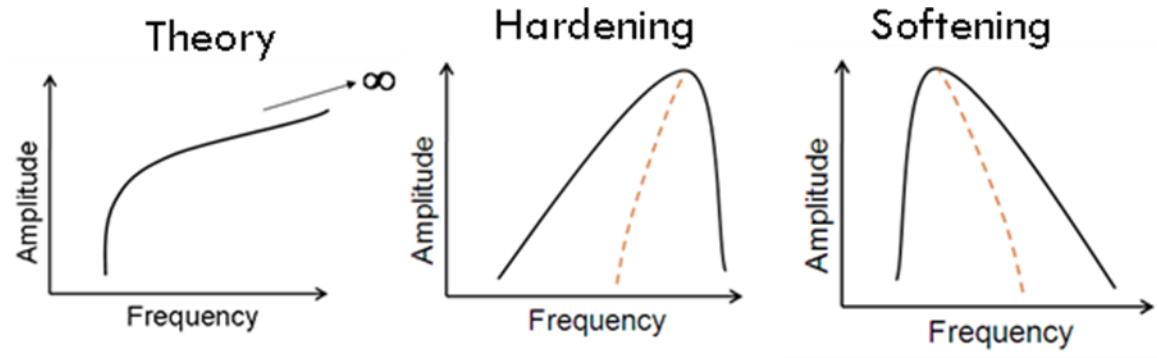

Figure 2.1. Response curve examples.

In previous works, experiments of this kind will include exciting the beam to a number of known frequencies and recording the amplitudes of each response. Thus, a relationship between vibration frequency and amplitude can be formed after numerous trials. Figure 2.2 shows results from [3] using this type of analysis. This work shall propose an alternative method of determining this relationship through the use of advanced digital signal processing and signal tracking methods. Furthermore, this method will also use free lateral vibration as opposed to forced axial vibration. This allows for the frequency-amplitude relationship to be found in a single experiment.

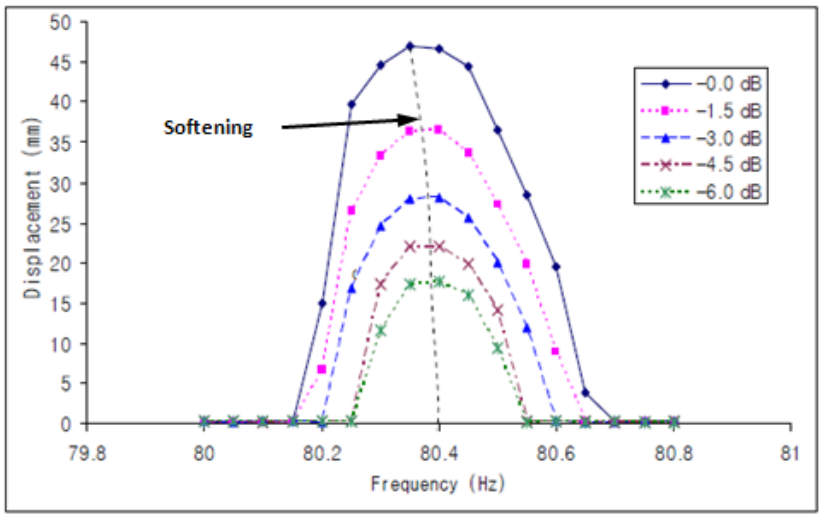

Figure 2.2. Experimental results from [3].

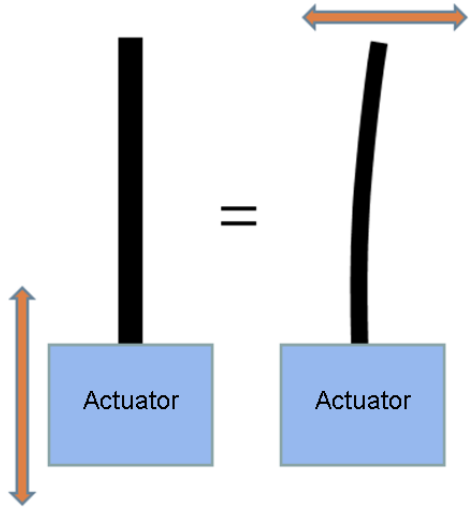

Figure 2.3. Sketch of parametric response of a cantilever beam.

2.2 Alternative Experimental Setup

As previously mentioned, the experiment which is being proposed will utilize free vibration of a cantilever beam. Two beams of lengths 0.782 m and 0.487 m have been chosen. Both have a width of 3.175 cm, a thickness of 0.3175 cm, and are made of cold rolled steel. In order to rid the effect of gravity on the beam's lateral vibrations, it was positioned in a completely horizontal orientation. A scanning laser vibrometer was

then focused on the beam and was also made level. For this experiment a Polytec PSV-200 laser vibrometer was utilized in conjunction with software which was controlled through a desktop computer. The beam was then physically pulled back a significant distance, released, and allowed to freely vibrate. Simultaneously, the laser vibrometer collected velocity measurements at a sampling frequency of 1.28 kHz. A sketch of this experimental setup can be seen in Fig. 2.4. In order to investigate the effects of gravity upon the beam's response, an experiment was also performed with the longer beam placed in a completely vertical position.

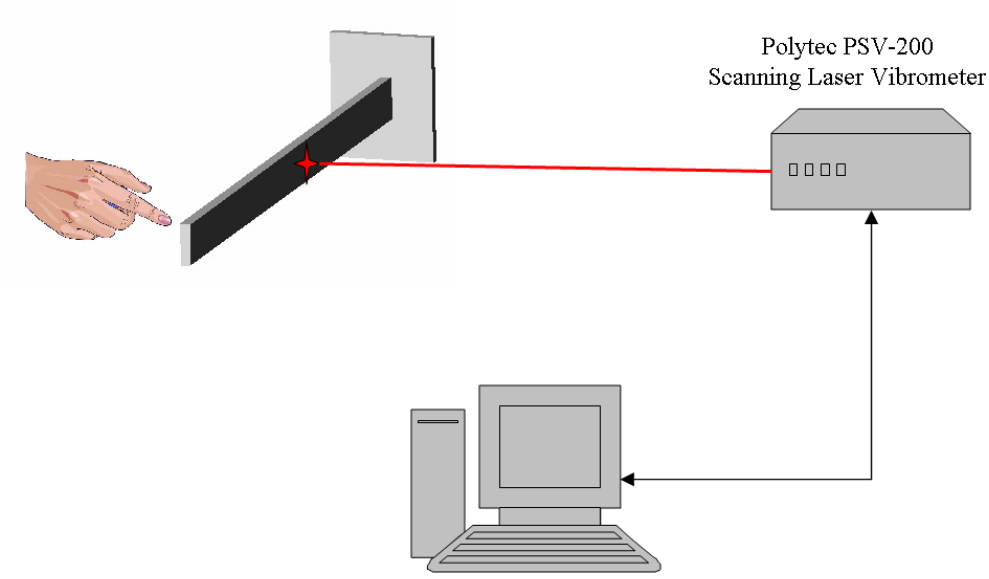

Figure 2.4. Sketch of experimental set up.

2.3 Experimental Results

For this experiment, two beams of different lengths were used. The longer beam had a length of 0.782 m and the shorter beam a length of 0.487 m. For the longer beam the laser was focused on a point 27.63 cm from the base, while for the shorter beam the

laser was located 28.42 cm from the base. Velocity profiles collected from the laser vibrometer for each beam in the horizontal position are shown in Fig. 2.5. Figure 2.6 gives the frequency domains for each of these velocity profiles which were obtained by using the fast Fourier transform. Figure 2.7 contains the velocity profile and frequency domain plot for the long beam in the vertical orientation. It can be seen from these profiles that the beams' vibration is composed of numerous modes, out of which mode one must be extracted for data analysis.

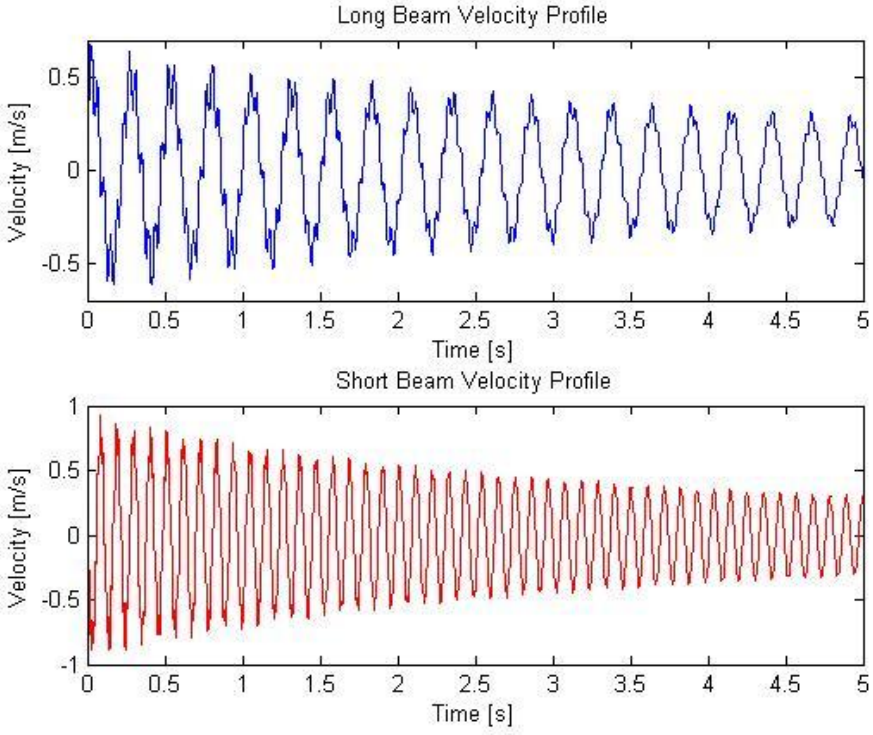

Figure 2.5. Horizontal beams' experimental velocity profiles

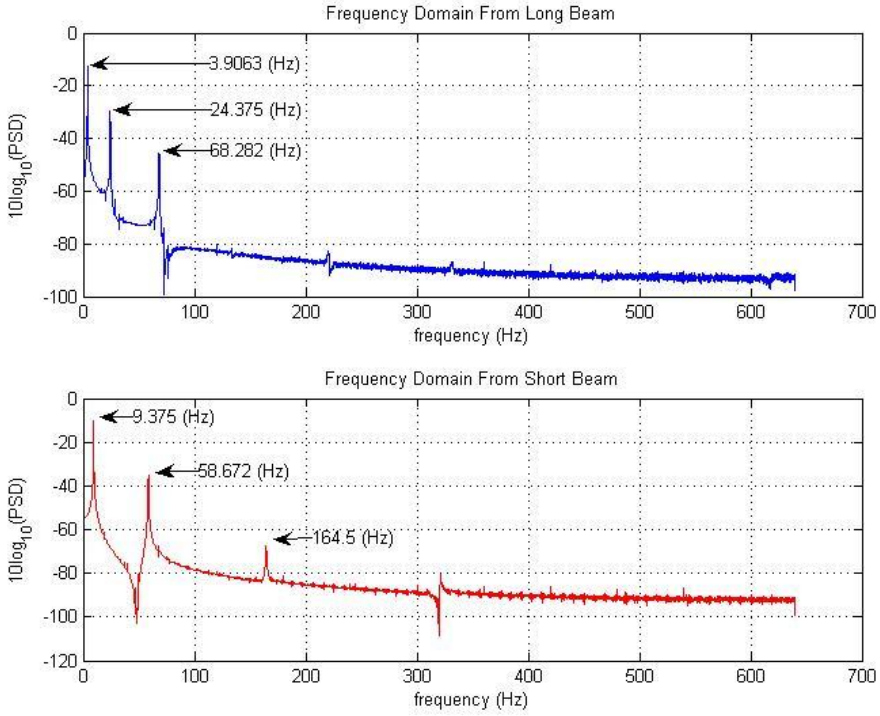

Figure 2.6. Horizontal beams' frequency domain plots

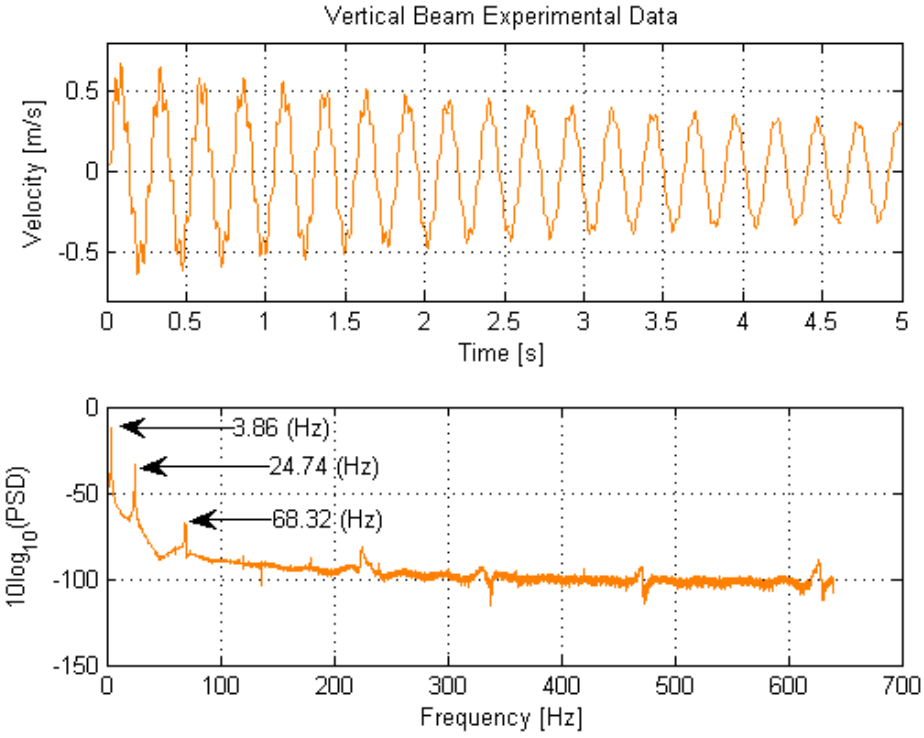

Figure 2.7. Vertical beam experimental data

Chapter 3 – Signal Processing

As it has been shown within the previous chapter, for this type of experiment the beam's vibration will be composed of numerous modes. It is necessary to extract from this data the mode which will be studied, i.e. mode one. Once the valuable data has been isolated, signal tracking methods will then be utilized for instantaneous frequency and amplitude calculations. For this work two different signal processing techniques have been used and compared for extracting the mode one vibration. They are a Butterworth 4th order low pass digital filter, and the empirical mode decomposition (EMD). In section 3.1 the low pass digital filter will be derived and two examples given. Within section 3.2, EMD will be described and an illustration of its use given.

3.1 Butterworth Low Pass Digital Filter

A low pass digital filter will be used to isolate mode one vibration from the experimental data. For this work a 4th order normalized Butterworth low pass filter has been used. The analog version of this filter takes the form seen in Eq. (3.1).

$$H(s)=\frac{1}{\left(s^2+\frac{3}{20}\sqrt{26}\cdot s+1\right)\cdot\left(s^2+\frac{181}{500}\sqrt{26}\cdot s+1\right)} \tag{3.1}$$

This form can be used for continuous analog signals or functions. The obtained experimental data has been collected using a constant sampling rate. Thus, it represents a discontinuous set of points. In order to use the filter described above, it must be transformed to a digital filter which can be used with discontinuous sets of data. After substituting Eq. (3.2) into the above equation for the low pass filter, setting

$\omega_{cc} = 1$, then substituting in Eq. (3.3) to map to the z-domain, Eq. (3.1) takes the form seen in Eq. (3.4).

$$s = \frac{s_{\omega_{cc}}}{\omega_{cc}} \tag{3.2}$$

$$s_{\omega_{cc}} = c\left[\frac{z-1}{z+1}\right] = c\left[\frac{1-z^{-1}}{1+z^{-1}}\right] \tag{3.3}$$

$$H(z) = \frac{1}{\left(c^2\left[\frac{1-z^{-1}}{1+z^{-1}}\right]^2 + \frac{3}{20}\sqrt{26}\cdot c\left[\frac{1-z^{-1}}{1+z^{-1}}\right]+1\right)\cdot\left(c^2\left[\frac{1-z^{-1}}{1+z^{-1}}\right]^2 + \frac{181}{500}\sqrt{26}\cdot c\left[\frac{1-z^{-1}}{1+z^{-1}}\right]+1\right)} \tag{3.4}$$

After some algebraic manipulation, the transfer function for the digital low pass filter in Eq. (3.4), becomes:

$$H(z) = \frac{Y(z)}{X(z)} = \frac{n_0 + n_1 z^{-1} + n_2 z^{-2} + n_3 z^{-3} + n_4 z^{-4}}{d_0 + d_1 z^{-1} + d_2 z^{-2} + d_3 z^{-3} + d_4 z^{-4}} \tag{3.5}$$

Expanding Eq. (3.5) using difference equations yields,

$$n_0 \cdot x(k) + n_1 \cdot x(k-1) + ... + n_4 \cdot x(k-4) = d_0 \cdot y(k) + d_1 \cdot y(k-1) + ... + d_4 \cdot y(k-4) \tag{3.6}$$

Now rearranging Eq. (3.6) to give the most recent output,

$$y(k) = \frac{n_0}{d_0}\cdot x(k) + \frac{n_1}{d_0}\cdot x(k-1) + ... + \frac{n_4}{d_0}\cdot x(k-4) - \frac{d_1}{d_0}\cdot y(k-1) - .... - \frac{d_4}{d_0}\cdot y(k-4) \tag{3.7}$$

Here *x(k)* is the incoming signal and *y(k)* represents the signal after being filtered. Within these equations the coefficients n_0 to n_4 and d_0 to d_4 are defined as:

$$n_0 = 1 \tag{3.7.1}$$

$$n_1 = 4 \tag{3.7.2}$$

$$n_2 = 6 \tag{3.7.3}$$

$$n_3 = 4 \tag{3.7.4}$$

$$n_4 = 1 \tag{3.7.5}$$

$$d_0 = \left[1 + c^2 + \frac{3\sqrt{26}}{20}c\right] \cdot \left[1 + c^2 + \frac{181\sqrt{26}}{500}c\right] \tag{3.7.6}$$

$$d_1 = \frac{4}{125}\left(1 - c^2\right)\left[125\left(1 + c^2\right) + 32\sqrt{26} \cdot c\right] \tag{3.7.7}$$

$$d_2 = \frac{1}{5000}\left[30000\left(1 - c^2\right) - 34118c^2\right] \tag{3.7.8}$$

$$d_3 = \frac{4}{125}\left(1 - c^2\right)\left[125\left(1 + c^2\right) - 32\sqrt{26} \cdot c\right] \tag{3.7.9}$$

$$d_4 = \left[1 + c^2 - \frac{3\sqrt{26}}{20}c\right] \cdot \left[1 + c^2 - \frac{181\sqrt{26}}{500}c\right] \tag{3.7.10}$$

In the above equations c is the warping coefficient defined as:

$$c = \cot\left(\frac{\omega_F \cdot T_s}{2}\right) \tag{3.7.11}$$

Within Eq. (3.7.11), T_s is the sampling period and ω_F is the highest frequency that the low pass filter will let pass. This design allows one to set ω_F just above the mode one frequency, thus filtering out all other mode vibrations.

Digital filters can be used to filter numerous dissimilar incoming signals and to remove random disturbances known as white noise from these more pure signals. Using a simple example it will be shown that a low pass filter can be used to separate two incoming signals.

Suppose that an incoming signal, *Y*, is composed of two other pure sinusoidal signals, y_1 and y_2. Signal y_1 will have an amplitude of 5 and a frequency of 8 Hz. Signal y_2 will have an amplitude of 2 and a frequency of 50 Hz. The complete incoming signal, *Y*, will be the sum of y_1 and y_2. Plots of y_1, y_2, and *Y* versus time can be seen in Figure 3.1.

$$Y = y_1 + y_2 \tag{3.8}$$

$$y_1 = 5\cos(2\pi 8t) \tag{3.8.1}$$

$$y_2 = 2\cos(2\pi 50t) \tag{3.8.2}$$

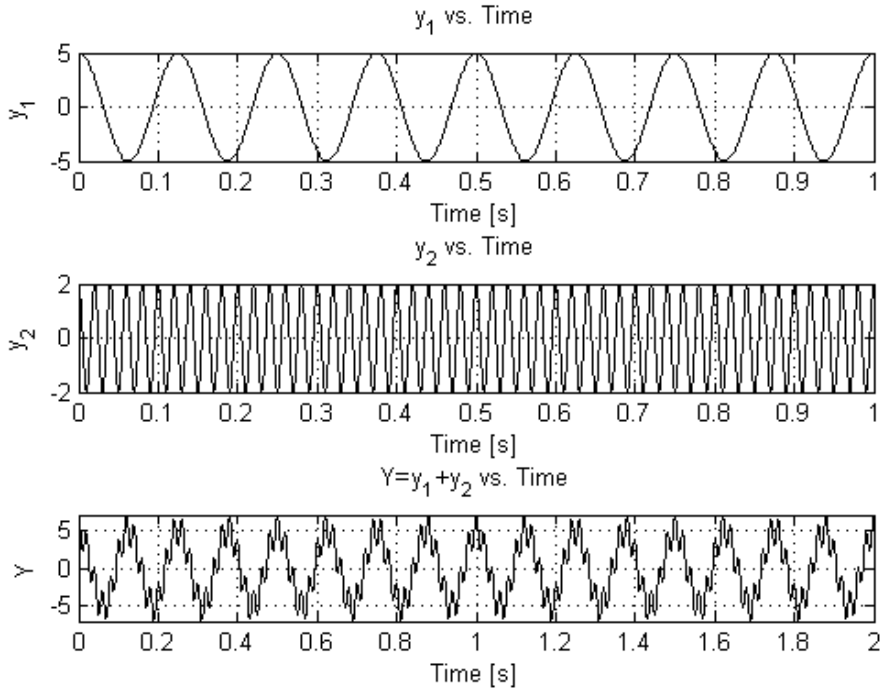

Figure 3.1. Plots y_1, y_2, and *Y* versus time

Utilizing the 4th order low pass filter described above, a MatLab m-file has been written to filter *Y* leaving just y_1. Here, the low pass limit was set 40% above the 8 Hz frequency of y_1 at 11.2 Hz. This file can be seen in Appendix A.1.1. Results from this example are shown in Figs. 3.2 – 3.3. Figure 3.2 displays the incoming signal and the

results after being filtered. Figure 3.3 again shows the incoming signal, *Y*, and the filtered signal. It also compares this with the original signal y_1, which was meant to be obtained through the use of the filter.

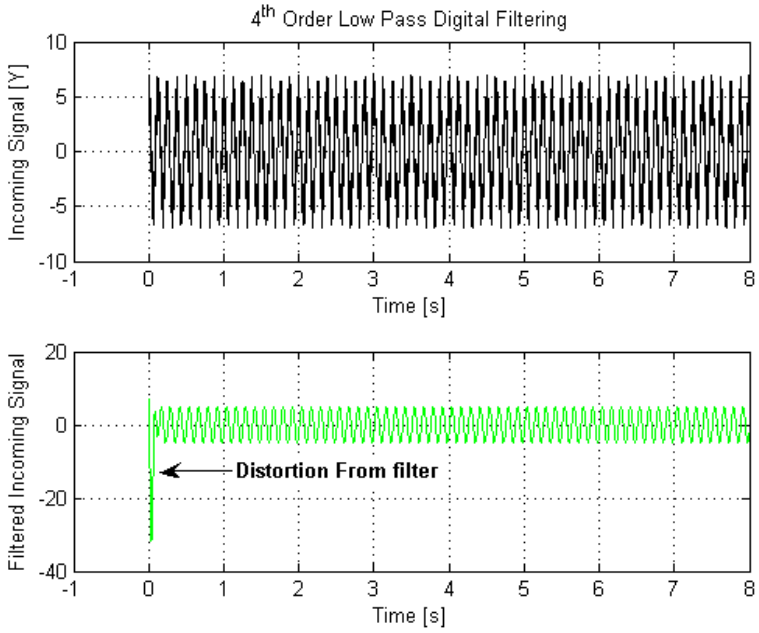

Figure 3.2. Plots showing *Y* before and after using a 4th order low pass digital filter

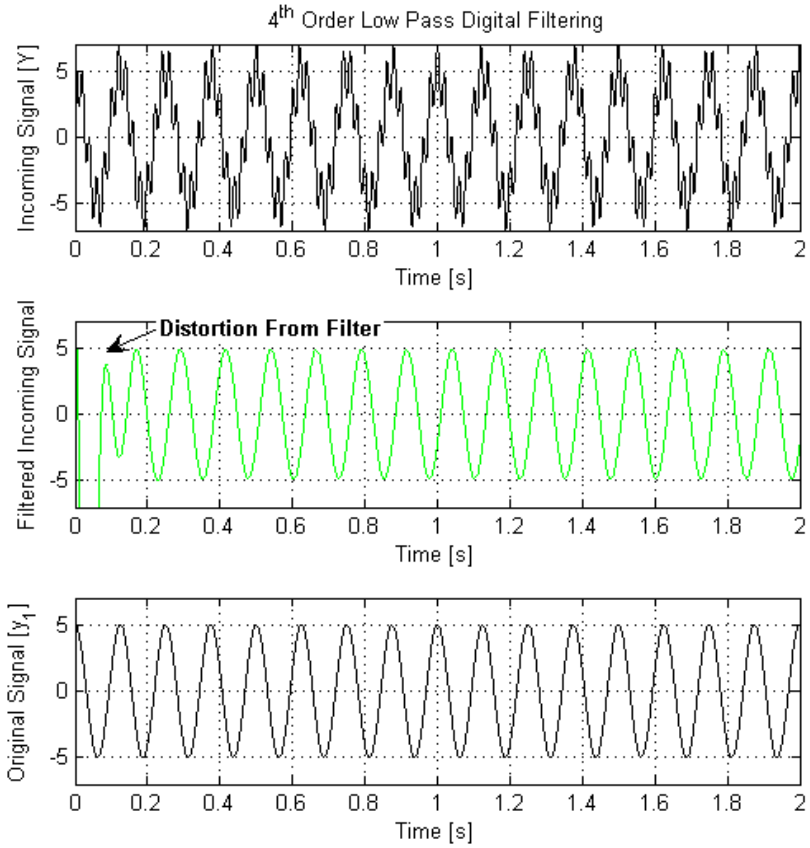

Figure 3.3. Plot of incoming signal, filtered incoming signal, and original signal, y_1

One adverse effect of using a digital filter is that there is a phase shift associated with the output of the filter. Also, the filter will distort the beginning of the incoming data which produces an "edge effect", known as the Gibbs phenomenon, at the beginning of the outputted data. This distortion can clearly be seen within Figs. 3.2 and 3.3. For this work, the beginning of the collected data will be the most valuable. In order to avoid this "edge effect" within this portion of the data, the signal will be fed through the filter backwards. This will prevent disturbing the most valuable data, but will ultimately alter the end of the data.

Using the same incoming signal, *Y*, and feeding it through the filter backwards gives the results found in Figs. 3.4 and 3.5.

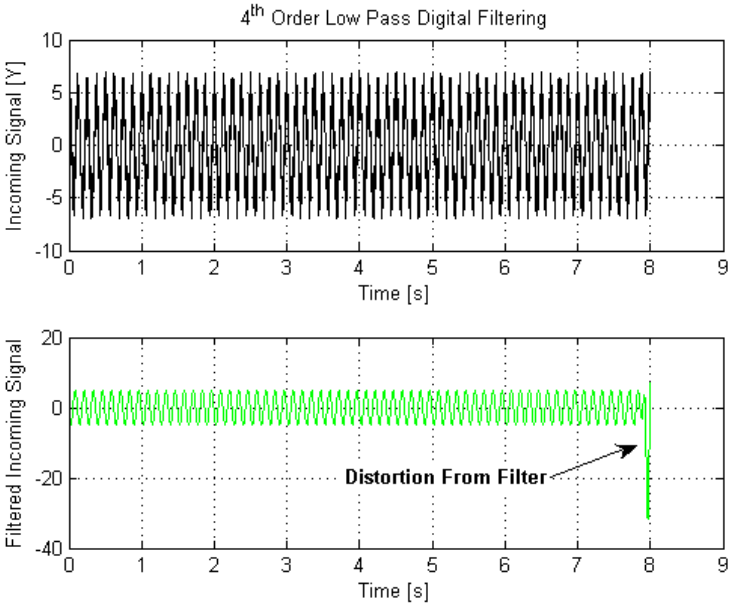

Figure 3.4. Results from filtering the incoming signal, *Y*, backwards

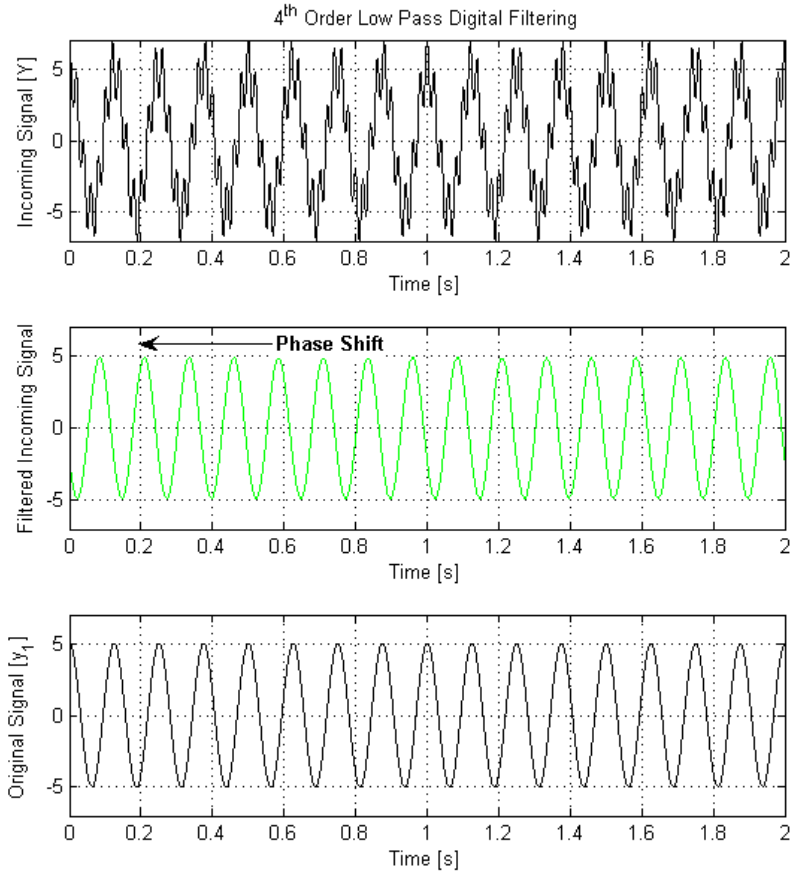

Figure 3.5. Incoming signal, backward filtered incoming signal, and original signal, y_1

Here the distortion from using the filter now occurs at the end of the incoming signal. Also, a small phase shift can clearly be seen as a result of using the filter. However, the amplitude and frequency of the filtered signal is nearly identical to the original y_1 signal. Thus, the filter is working to reduce the total incoming signal Y to just y_1. It should be noted that when utilizing the low pass filter on the obtained experimental data, the disturbed portion has been ignored within further signal tracking analysis.

Another application of the low pass digital filter is the removal of additional random signals known as white noise. To illustrate this, an incoming signal described through Eqs. (3.9) – (3.9.1) will be used as an example. Here, Y will refer to the

summation of signal y_1 and white noise. The additional white noise will be generated by using MatLab's "unf*rnd*" command. Again, the same 4th order low pass filter will be used to filter out the additional white noise added to signal y_1. The incoming signal will also be fed through the filter backwards to show the distorted region at the end of the data. The MatLab program used for this example can be seen in appendix A.1.2 and Figs. 3.6 – 3.8 display the results.

$$Y = y_1 + White\ \ Noise \tag{3.9}$$

$$y_1 = 5\cos(2\pi 8t) \tag{3.9.1}$$

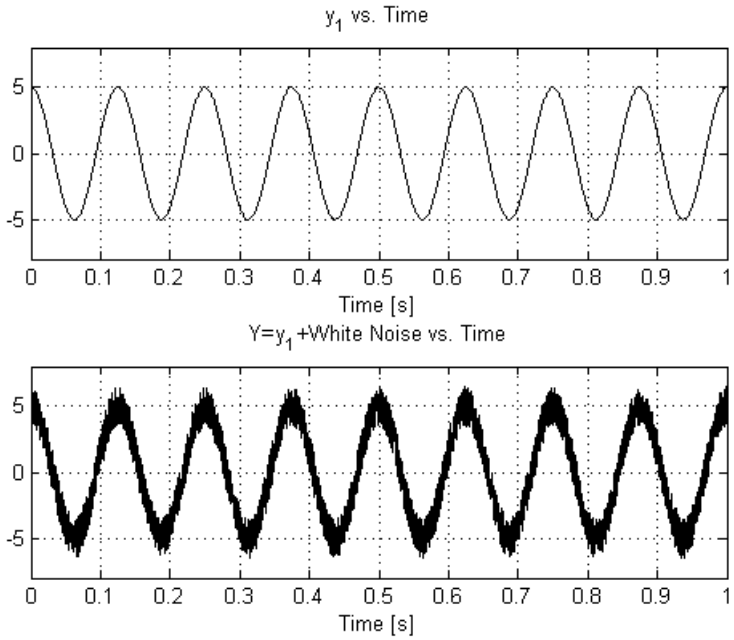

Figure 3.6. Plot of y_1 before and after additional white noise

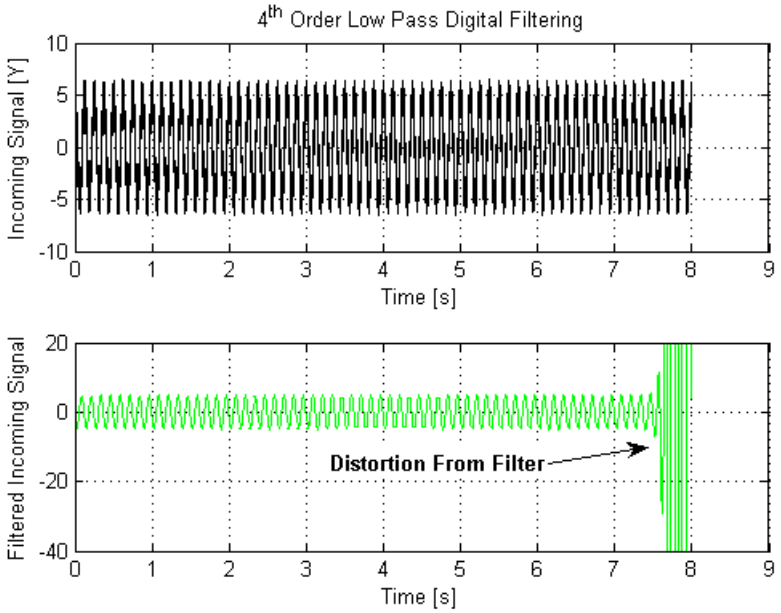

Figure 3.7. Plots of *Y* before and after the 4th order low pass digital filter

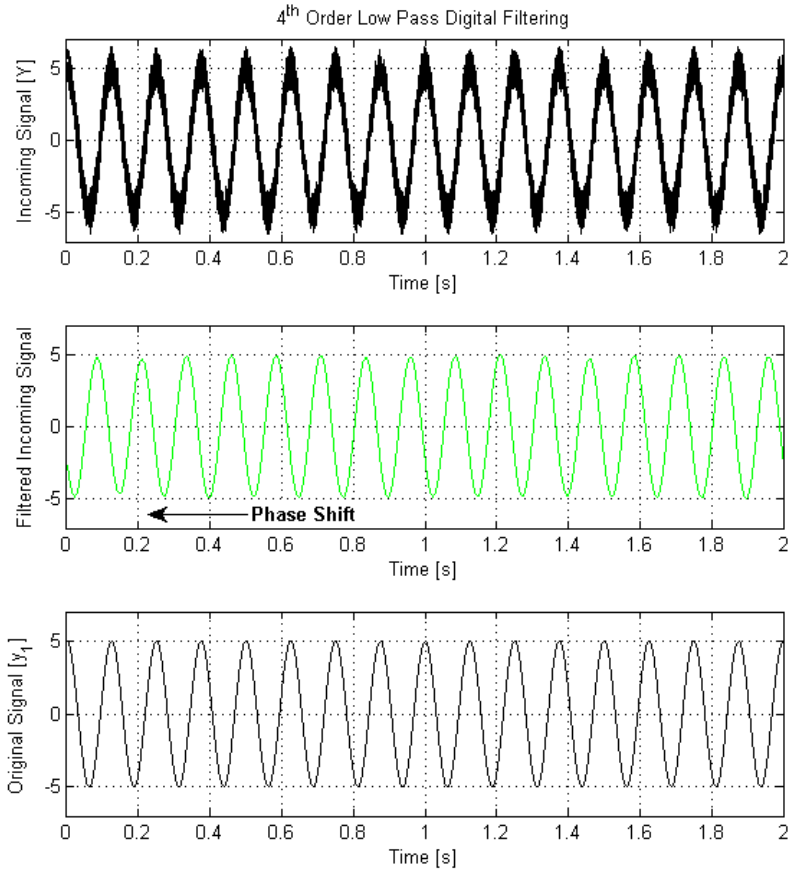

Figure 3.8. Plot of incoming signal, filtered incoming signal, and original signal, y_1

Figure 3.6 shows signal y_1 before and after the addition of white noise. Figure 3.7 displays signal y_1 with the addition of white noise and the results after being filtered using the 4^{th} order low pass filter. Again the distortion from using the filter can be seen. However, because the incoming signal was processed through the filter backwards, the disturbed region is located near the end of the data. These results are again plotted within Fig. 3.8 in addition to the original y_1 signal for comparison. Again a small phase shift can be seen, however the additional white noise has been virtually completely removed from the signal.

3.2 Empirical Mode Decomposition

Empirical mode decomposition (EMD) is another signal processing technique that will extract all intrinsic mode functions (IMFs) from a signal. An IMF is defined as a signal which can be characterized by the following two definitions found in [4].

(1) The number of extrema and the number of zero crossings of the function must be equal or differ by at most one.

(2) At any point of the function, the mean value of the envelopes defined by the local extrema should be zero.

Thus, EMD can be used to extract all vibration modes from the data collected by the laser vibrometer. EMD uses what is known as the "sifting process" to accomplish this. The sifting process is as follows. Consider a signal *Y(t)*. First, the local maxima of the signal are found and connected using a natural cubic spline. The local minima are then found and also connected using a natural cubic spline. The mean of these two

envelopes will be designated as m_1. This mean is then subtracted from *Y(t)* forming the first component h_1.

$$h_1 = Y(t) - m_1 \tag{3.10}$$

Then local maxima and minima of h_1 are then found and are again connected using cubic splines. The mean of these two envelopes is calculated and subtracted from h_1. This process continues *k* number of times until the mean of the two envelopes is close to zero. Then the *k* component, h_k, is now the first extracted IMF, c_1.

$$h_k = c_1 \tag{3.11}$$

The first IMF, c_1, is now subtracted from *Y(t)* and the sifting process repeats on this remaining part of the original signal until all IMFs are extracted from *Y(t)*. EMD may still result in some Gibbs Phenomenon. The cubic spline at the end or the beginning of the data range may distort the isolated IMF by trying to join to this first or last data point as it will connect to all local extrema. However, unlike the digital filter these edge effects can be avoided through a technique which extends the spline past the last available extremum and existing data. A full derivation and explanation of EMD can be seen within [5].

To illustrate an example of how EMD uses this sifting process to extract all IMFs, consider the example found in section 3.1 through Eqs. (3.8) – (3.8.2). The incoming signal, *Y*, is composed of two pure signals with different amplitude and frequencies. First the local minima and maxima are found and connected using a cubic spline, as seen in Fig. 3.9.

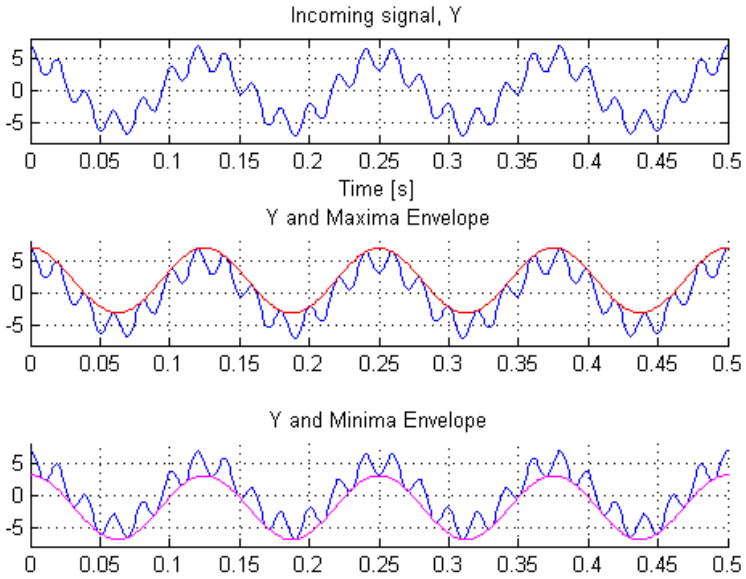

Figure 3.9. EMD analysis, *Y* with maxima and minima envelopes

The mean of these two envelopes are found, forming m_1. This mean is then subtracted from the original signal forming the first component h_1. Figure 3.10 shows the original signal with the two envelopes, their mean, and h_1. Here it can be seen that even after this first sifting process, h_1 begins to take a form very similar to y_2.

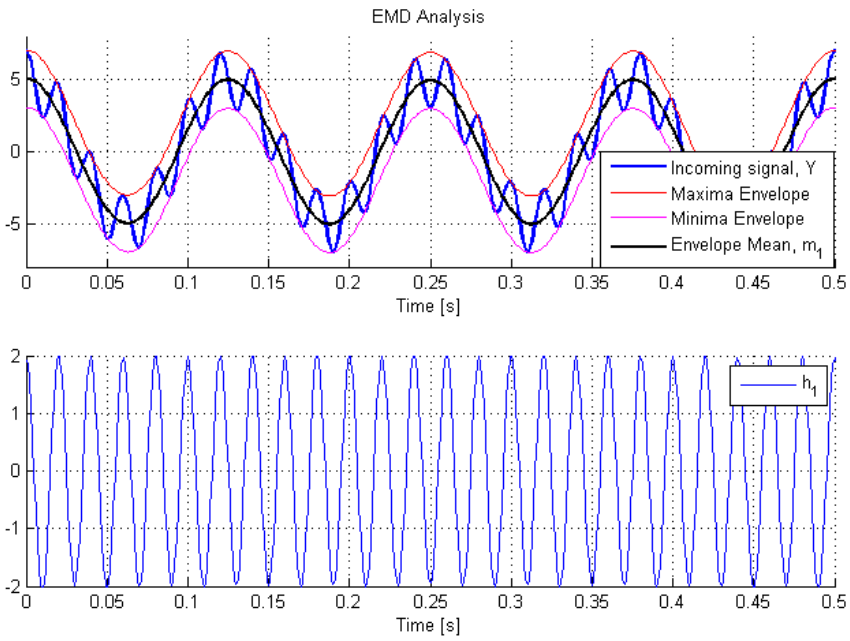

Figure 3.10. EMD analysis, first sifting pass resulting in h_1

The sifting process is then repeated numerous times until the mean of the two envelopes approaches zero, resulting in the first extracted IMF, c_1. The first IMF is then subtracted from the original signal, *Y*, and the sifting process continues again until the second IMF, c_2, is isolated. Figure 3.11 displays the final results of EMD analysis of this example. Here, when compared to Fig. 3.1, it can be seen that c_1 and c_2 are virtually identical to the original y_1 and y_2 components. Furthermore, there is no phase shift associated with the results of the EMD sifting process.

Using this algorithm, all modes of vibration can be isolated from the cantilever beam experimental data. Thus, mode one can be accurately acquired from the experimental data for signal tracking analysis.

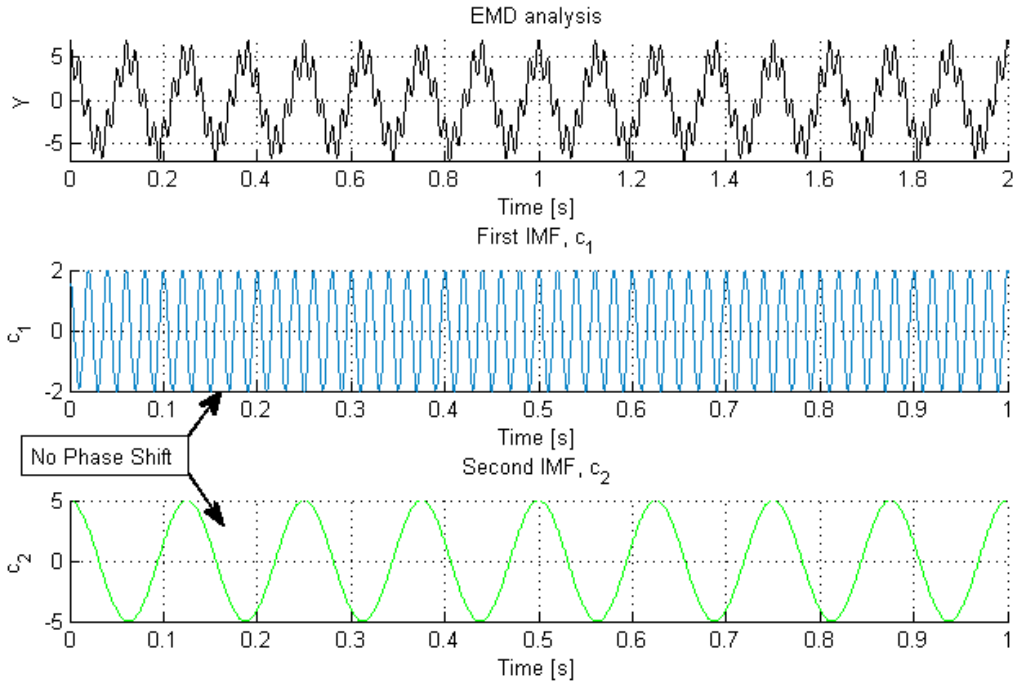

Figure 3.11. EMD analysis, incoming signal ,*Y*, with extracted IMFs, c_1 and c_2

Chapter 4 – Signal Tracking

Within this work, an alternate method for collecting data and determining the nonlinear characteristics of the dynamic response of a vibrating structure is proposed. This method utilizes free transient vibrations in contrast to forced steady state responses. The relationship between the instantaneous frequency and amplitude of the structures response is of interest. In particular, defining this nonlinear relationship as hardening or softening is necessary.

As shown in chapter 2, the raw experimental data contains numerous modes of vibration. Mode one vibration will be the target of interest, thus it must be isolated from the other modes. In order to accomplish this, the two signal processing techniques described in chapter 3 have been used. They are the 4^{th} order low pass digital filter and the empirical mode decomposition. Once mode one has been extracted, the instantaneous frequency and amplitude of this signal will be calculated by utilizing three separate signal tracking methods. These three methods are the Teager-Kaiser algorithm (TKA), the Hilbert-Huang transform (HHT), and the harmonics tracking method (HTM). TKA and HHT are two well known and previously used signal tracking techniques. Recently, a novel signal tracking method, HTM, has been proposed as an additional tool for signal analysis. All three signal tracking methods will be used in conjunction with both signal processing techniques to determine the instantaneous frequency and amplitude. The results of all will then be compared.

Sections 4.2 – 4.3 will describe all three signal tracking techniques TKA, HHT, and HTM respectively. In section 4.4, and example of a nonlinear system, a nonlinear

damped pendulum, will be used to validate the use of and compare the results of each method.

4.1 The Teager-Kaiser Algorithm

In order to calculate the instantaneous frequency and amplitude of an incoming signal, the Teager-Kaiser algorithm (TKA) uses four recent data points and a product known as the energy of harmonic oscillation, $a^2\omega^2$. This value is defined in Eq. (4.1) and is seen again in Eq. (4.2)

$$\begin{aligned}\Psi(u) &= [u'(t)]^2 - u(t)u''(t) \\ &= a^2\omega^2\end{aligned} \tag{4.1}$$

$$\begin{aligned}\Psi(u') &= [u''(t)]^2 - u'(t)u'''(t) \\ &= a^2\omega^4\end{aligned} \tag{4.2}$$

Here, *u(t)*, is a function which describes the incoming signal. For this experiment, *u(t)*, is a collection of data points and is not a clearly defined function. Hence, *u(t)* will be estimated using cubic polynomial interpolation. Using the previous equations, the instantaneous amplitude and frequency can now be calculated with Eqs. (4.3) and (4.4).

$$a(t) = \frac{\Psi(u)}{\sqrt{\Psi(u')}} \tag{4.3}$$

$$\omega(t) = \sqrt{\frac{\Psi(u')}{\Psi(u)}} \tag{4.4}$$

The Teager-Kaiser algorithm is simple and effective for many types of functions, however many incoming digital signals, represented here as *u(t)*, are not clearly defined by simple functions such as sine or cosine. During this experiment, for example, data is

collected using the laser vibrometer which takes readings at a specific sampling rate. For these types of situations there is no clearly defined function, *u(t)*, which represents this data. For this circumstance the data points may be curve fitted using a numerical method known as cubic polynomial interpolation. Using this method it is possible to create a polynomial which defines the data obtained through the sampling experiment.

Consider a case where data points have been collected using the sampling rate, T_s. It is desired to curve fit these data points in order to obtain a function, *u(t)*¸which describes this set of data. Figure 4.1 shows an example where four known data points have been collected and plotted: $(-3T_s/2, u_1)$, $(-T_s/2, u_2)$, $(T_s/2, u_3)$, and $(3T_s/2, u_4)$.

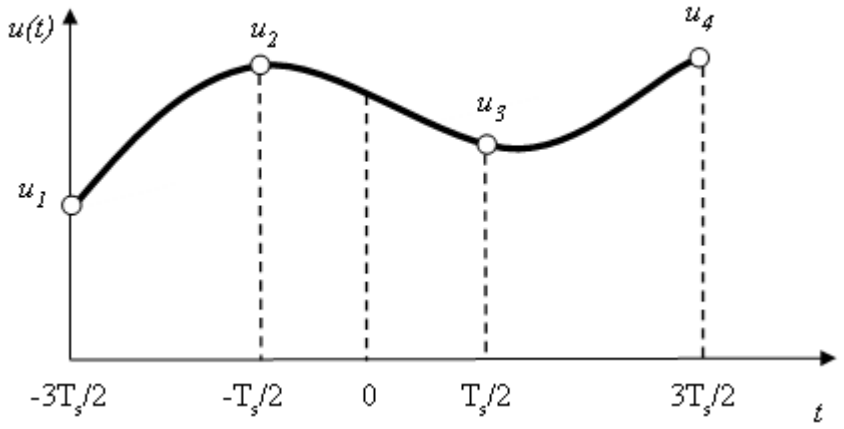

Figure 4.1. Cubic interpolation example

In the general case, the cubic polynomial, *u(t)*, will take the form:

$$u(t) = C_0 + C_1 t + C_2 t^2 + C_3 t^3 \tag{4.5}$$

$$u(0) = C_0 \tag{4.6}$$

$$u'(0) = C_1 \tag{4.7}$$

$$u''(0) = 2C_2 \tag{4.8}$$

$$u'''(0) = 6C_3 \tag{4.9}$$

Using the four known data points and the general polynomial form, the system can be expressed in matrix form.

$$\mathbf{U} = \mathbf{M} \cdot \mathbf{C} \tag{4.10}$$

$$\begin{bmatrix} u_1 \\ u_2 \\ u_3 \\ u_4 \end{bmatrix} = \begin{bmatrix} 1 & \frac{-3T_s}{2} & \left(\frac{-3T_s}{2}\right)^2 & \left(\frac{-3T_s}{2}\right)^3 \\ 1 & \frac{-T_s}{2} & \left(\frac{-T_s}{2}\right)^2 & \left(\frac{-T_s}{2}\right)^3 \\ 1 & \frac{T_s}{2} & \left(\frac{T_s}{2}\right)^2 & \left(\frac{T_s}{2}\right)^3 \\ 1 & \frac{3T_s}{2} & \left(\frac{3T_s}{2}\right)^2 & \left(\frac{3T_s}{2}\right)^3 \end{bmatrix} \cdot \begin{bmatrix} C_0 \\ C_1 \\ C_2 \\ C_3 \end{bmatrix} \tag{4.11}$$

Solving for coefficients C_0, C_1, C_2, and C_3.

$$\mathbf{U} \cdot \mathbf{M}^{-1} = \mathbf{C} \tag{4.12}$$

$$\begin{bmatrix} u_1 \\ u_2 \\ u_3 \\ u_4 \end{bmatrix} \cdot \begin{bmatrix} -1/16 & 9/16 & 9/16 & -1/16 \\ 1/24T_s & -27/24T_s & 27/24T_s & -27/24T_s \\ 1/4T_s^2 & -1/4T_s^2 & -1/4T_s^2 & 1/4T_s^2 \\ -1/6T_s^3 & 3/6T_s^3 & -3/6T_s^3 & 1/6T_s^3 \end{bmatrix} = \begin{bmatrix} C_0 \\ C_1 \\ C_2 \\ C_3 \end{bmatrix} \tag{4.13}$$

Thus,

$$u(0) = C_0 = \frac{1}{16}\left(-u_1 + 9u_2 + 9u_3 - u_4\right) \tag{4.14}$$

$$u'(0) = C_1 = \frac{1}{24T_s}\left(u_1 - 27u_2 + 27u_3 - u_4\right) \tag{4.15}$$

$$u''(0) = 2C_2 = \frac{1}{2T_s^2}\left(u_1 - u_2 - u_3 + u_4\right) \tag{4.16}$$

$$u'''(0) = 6C_3 = \frac{1}{T_s^3}\left(-u_1 + 3u_2 - 3u_3 + u_4\right) \tag{4.17}$$

The coefficients of the cubic polynomial, *u(t),* have been solved for and now this function can be used within the Teager-Kaiser algorithm in order to find the instantaneous amplitude and frequency of the collected data.

4.3 The Hilbert-Huang Transform

Prior to the existence of the Hilbert-Huang Transform (HHT), signal analysis methods were limited to linear or stationary system assumptions. As is well known, the majority of physical systems occurring in nature are neither stationary nor linear. Thus, the need for an advanced signal analysis tool which can determine characteristics of a system which is nonlinear and non-stationary is in great demand. Modern attempts have been made to create such a tool. However, each deals with either a nonlinear or a non-stationary signal, but not both simultaneously. The development of HHT brought forth the ability to evaluate nonlinear and non-stationary signals. This transform takes the form in (4.18). Here *x(t)* is the incoming signal which will be evaluated. *PV* represents the Cauchy prime value of the singular integral and τ is a time delay.

$$y(t) = H\left[x(t)\right] = \frac{1}{\pi} PV \int_{-\infty}^{\infty} \frac{x(\tau)}{t-\tau} d\tau \tag{4.18}$$

Through the use of this transform, the analytical signal then takes the form in Eq. (4.19).

$$z(t) = x(t) + iy(t) = a(t)e^{i\theta(t)} \tag{4.19}$$

Here *a(t)* is the instantaneous amplitude of the signal *x(t)* and $\theta(t)$ is the phase function, which are defined below.

$$a(t) = \sqrt{x^2 + y^2} \tag{4.20}$$

$$\theta(t) = \arctan\left(\frac{y}{x}\right) \tag{4.21}$$

The instantaneous frequency of *x(t)*, *ω(t)*, is then defined are the derivative of θ*(t)* with respect to time, as seen in (4.22).

$$\omega(t) = \frac{d\theta}{dt} \tag{4.22}$$

Once the pertinent information has been isolated from the experimental data, either by using EMD or the low pass digital filter, HHT can then be utilized for instantaneous frequency and amplitude calculations.

4.2 The Harmonics Tracking Method

The harmonics tracking method (HTM) is a newly developed signal analysis tool which can also evaluate nonlinear and non-stationary signals. HTM can also be used to extract amplitude and frequency data from an incoming signal. HTM has proven in [6] to be robust to signals with moving averages and noise, while using only three recent data points. HTM assumes that the signal being considered will take the following form,

$$\begin{aligned} u(t) &= C_0 + e_1 \cos(\omega t) - f_1 \sin(\omega t) \\ &= C_0 + C_1 \cos(\omega \bar{t}) - D_1 \sin(\omega \bar{t}) \end{aligned} \tag{4.23}$$

Here, C_0, e_1, and f_1 are unknown constants. Also, $\bar{t}\left(\equiv t - t_n\right)$ is a localized time coordinate where t_n is the current time. The coefficients C_1 and D_1 then take the form in (4.24) and (4.25).

$$C_1 = \sqrt{e_1^2 + f_1^2} \tag{4.24}$$

$$D_1 = \sqrt{e_1^2 + f_1^2}\sin\left(\omega t_n + \phi_1\right)$$

$$\phi_1 = \arctan\left(\frac{f_1}{e_1}\right) \tag{4.25}$$

HTM utilizes TKA for an initial guess of the signal frequency at the third data point, thus HTM starts frequency tracking after the fourth data point. After this point the previous point's frequency will be used as an initial guess to the current point's frequency. From this, the unknowns C_0, C_1, and D_1 for each current data point, when $\bar{t} = 0$ or $t = t_n$, can be found by minimizing the square error.

$$E_{error} = \sum_{i=0}^{-m+1} \alpha^{|i|}\left(u_{n+i} - \bar{u}_{n+1}\right)^2 \tag{4.26}$$

Here u_{n+i} signifies the second part of Eq. (4.23) with $\bar{t} \equiv \bar{t}_i = i\Delta t$. Also, $\bar{u}_{n+i}$ is *u(t)* at $t = t_n + \bar{t}_i$. Once these constants are found, the instantaneous amplitude and frequency can be determined by utilizing Eqs. (4.27) – (4.29). A complete derivation of HTM can be seen in [6].

$$a \equiv \sqrt{C_1^2 + D_1^2} = \sqrt{e_1^2 + f_1^2} \tag{4.27}$$

$$\theta = \arctan\left(\frac{D_1}{C_1}\right) = \omega t_n + \phi_1 \tag{4.28}$$

$$\omega = \frac{d\theta}{dt} \tag{4.29}$$

4.4 Validation and Comparison of Signal Tracking Methods

In order to validate the use of and as a comparison of results, an example of a nonlinear system which is frequency and amplitude dependent will be analyzed. The

well known nonlinear damped pendulum, which can be described through Eq. (4.22), will be used.

$$\ddot{\theta} = -\frac{g}{L}\sin(\theta) - \frac{\gamma}{m}\dot{\theta} \tag{4.22}$$

In the above equation *g*, *L*, *m*, γ represent gravity, length of pendulum, mass, and dampening ratio respectively. The angle at which the pendulum is swinging, θ, is the unknown variable. A MatLab program has been written which simulates the transient response of the damped pendulum. This program, which can be seen in Appendix A.2, utilizes MatLab's "ode113" command, and the values found in Table 1. The results of which can be seen through Figs. 4.2 – 4.5.

Table 4.1. Values used in damped pendulum simulation

Variable	Value
g	9.81 m/s^2
L	0.1 m
m	5 kg
γ	0.3

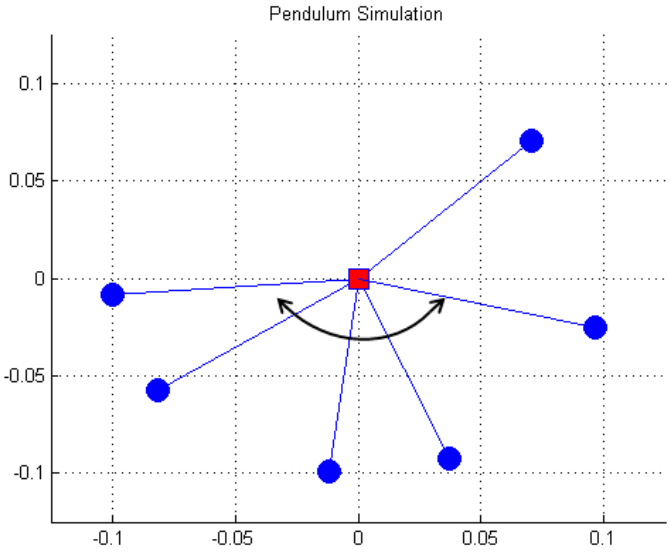

Figure 4.2. MatLab Pendulum Simulation

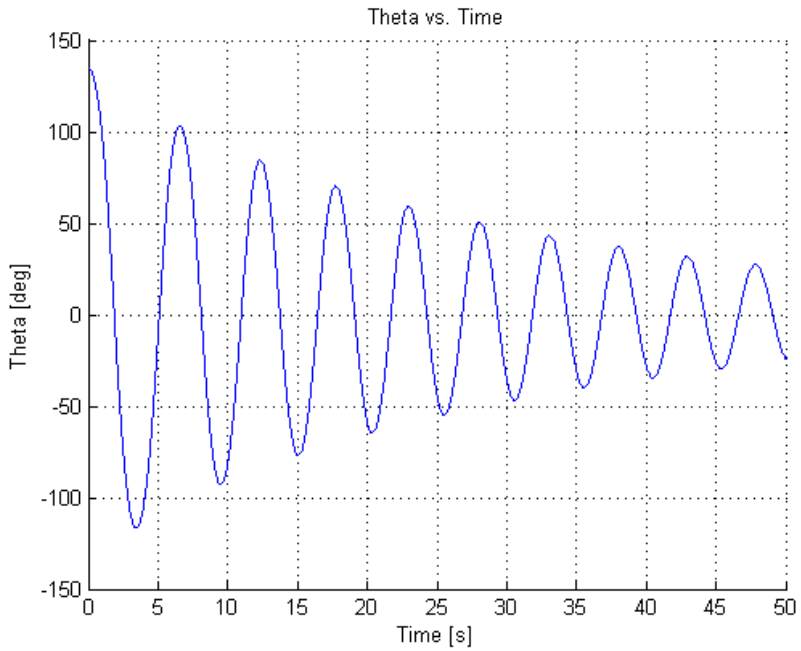

Figure 4.3. Pendulum simulation results, Theta vs. Time

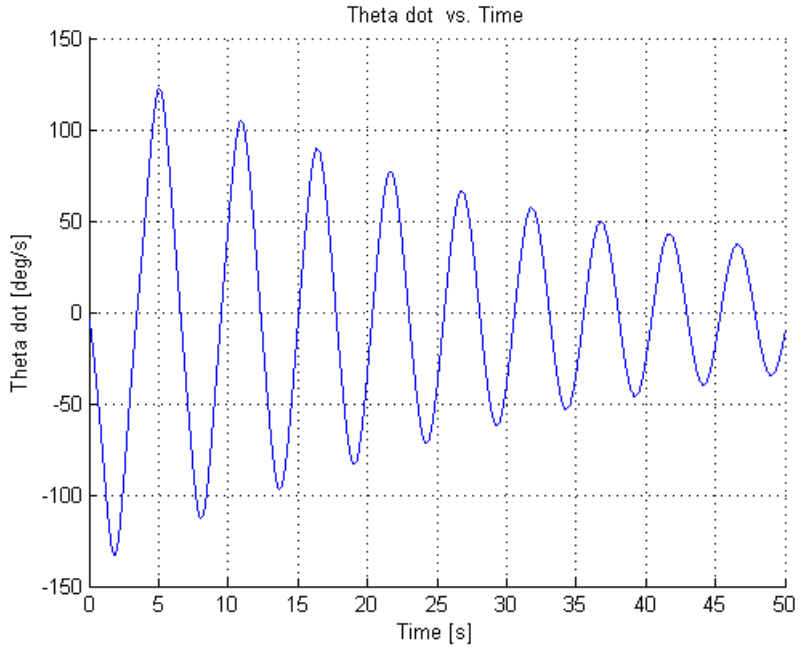

Figure 4.4. Pendulum simulation results, Theta dot vs. Time

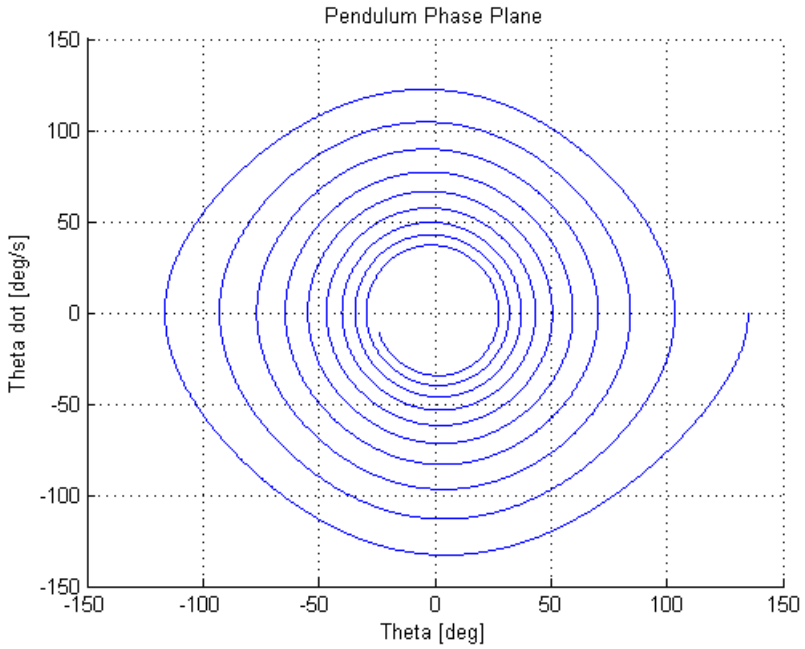

Figure 4.5. Pendulum simulation results, Phase Plane Diagram

By utilizing the signal tracking techniques, the instantaneous amplitude and frequency of the pendulum simulation data can be calculated. The difference in results of each can clearly be seen. Figure 4.6 displays the results obtained through the Teager-Kaiser algorithm, while Figs. 4.7 – 4.8 show results from the Harmonics Tracking Method and the Hilbert-Huang transform.

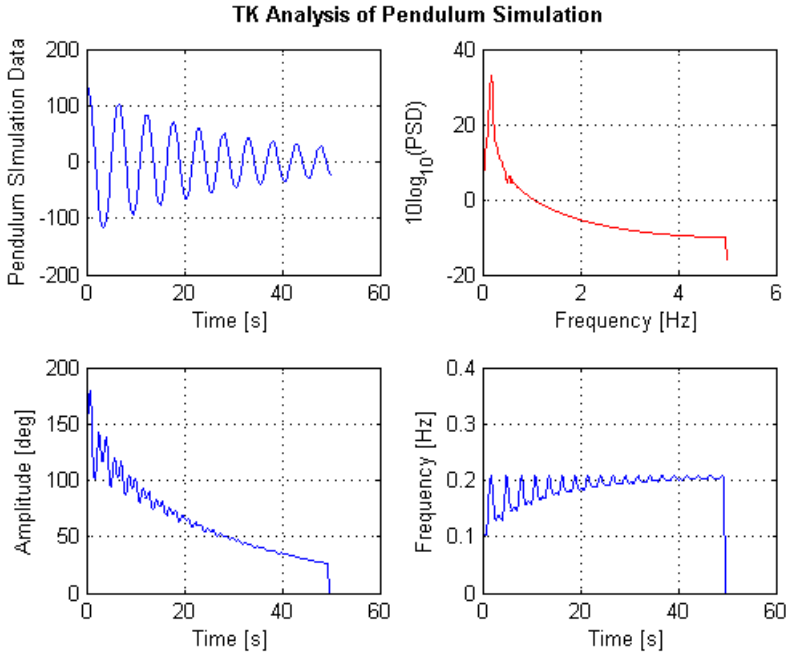

Figure 4.6. TK analysis of pendulum simulation

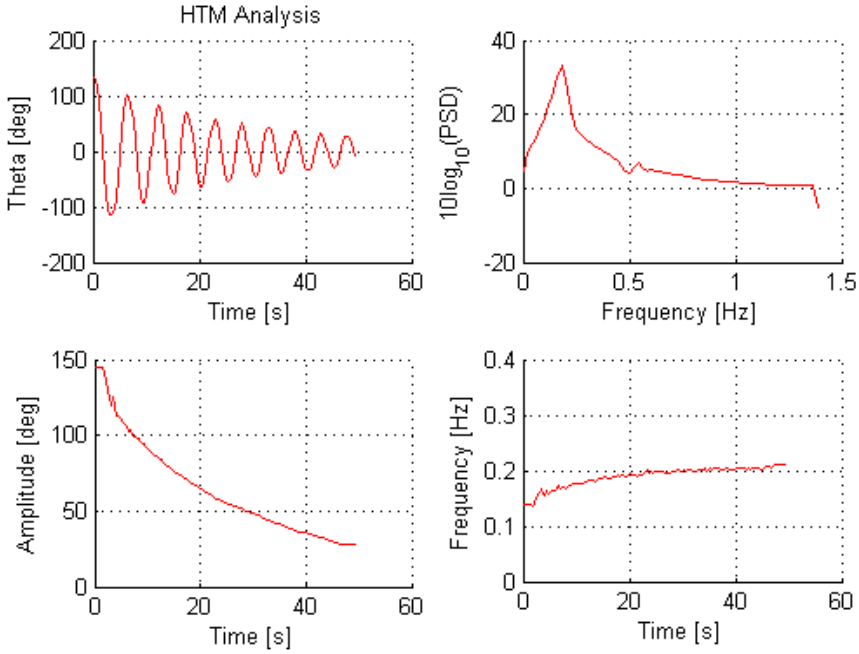

Figure 4.7. HTM analysis of pendulum simulation

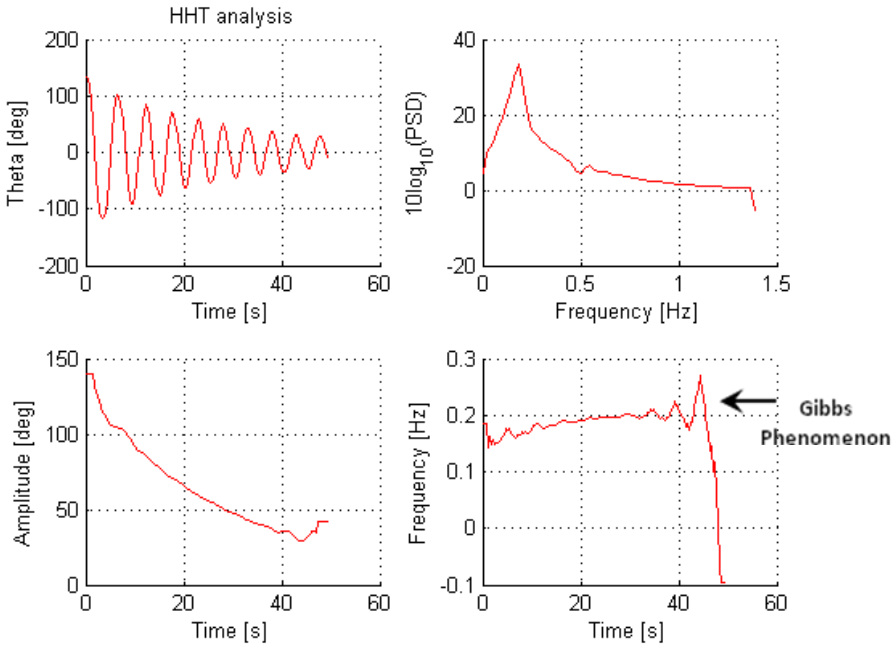

Figure 4.8. HHT analysis of pendulum simulation

From these figures it can be seen that HTM provides the clearest data with little distortions. TKA, while the simplest signal tracking method, offers data which displays a general trend but with little accuracy. In contrast to HTM and TKA, the data from HHT is clear in the midsection of the data set, but large distortions near the beginning and end of the data, known as Gibbs phenomenon, can be seen.

Taking the data after HTM analysis and plotting the instantaneous frequency versus amplitude clearly shows a downward sloping trend which indicates a softening response. Figure 4.9 presents a plot of this data which has been curve fitted using a second order polynomial least-squares fit. From the fit equation, the negative coefficient on the nonlinear term also indicates a softening effect.

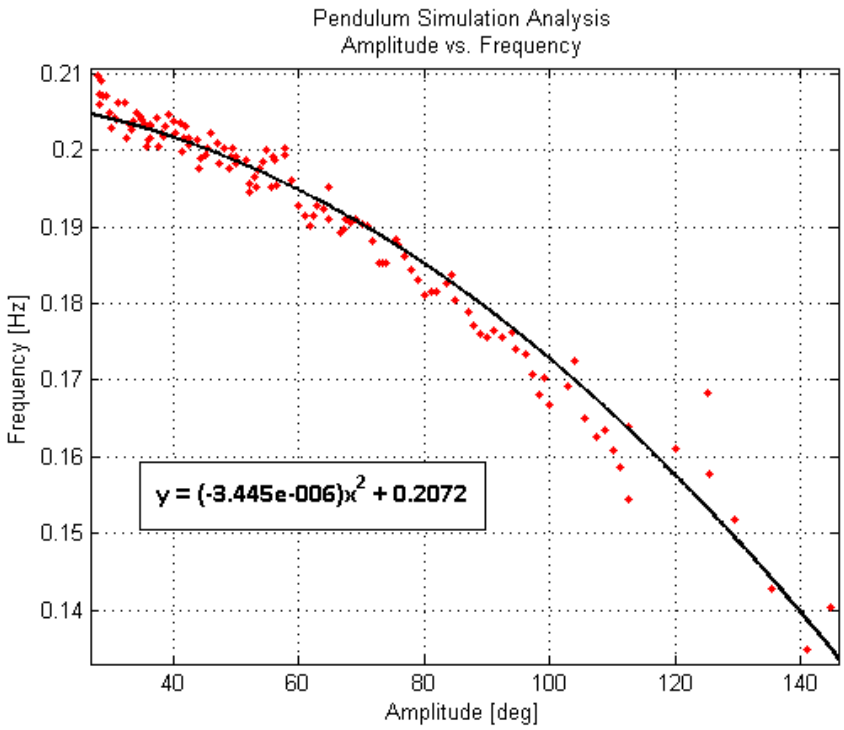

Figure 4.9. Pendulum simulation, HTM amplitude vs. frequency

Through this example one can easily see how these signal tracking methods can be used to determine nonlinearity. Analogous to the cantilever beam experiment, it is desired to obtain the sign and amplitude of this nonlinear coefficient to determine hardening or softening and the strength of nonlinearity within the system.

Through the example, which represents an optimal set of data with no distortions from signal processing or noise, the strengths and weaknesses of each technique can be seen. TKA has less resolution and accuracy when compared to both HTM and HHT, however does not contain edge effects. HHT, although containing little fluctuations within the midsection of its frequency data, has large edge effects which distort the most valuable of information. HTM, in contrast to each, contains no edge effects and little fluctuations throughout the instantaneous amplitude and frequency data sets.

Chapter 5 – Experimental Data Processing and Tracking Results

As described in chapter 2, an experiment was performed which collected data from the free transient vibration of a cantilever beam. Two beams of different lengths were placed in the horizontal position, set in motion, and allowed to freely vibrate as data was collecting using a laser vibrometer. The longer beam was then vertically oriented and the experiment repeated.

When processing the experimental data, numerous methods were utilized. The first step in processing is to extract mode one from the pure experimental data. A 4^{th} order low pass digital filter or EMD were used to accomplish this. From this data, the instantaneous amplitude and frequency of the signal was obtained through the use of HTM, HHT, or TKA. This process was done for both sets of horizontal beam data, which produces twelve sets of results which are then compared. Similarly, the same algorithm was used to process the data from the vertical beam experiment for a total of eighteen sets of results. Figure 5.1 is a flow chart which visualizes this logic. Sections 5.1 – 5.3 will present the signal processing and tracking results for the horizontal long beam, the horizontal short beam, and the vertical long beam.

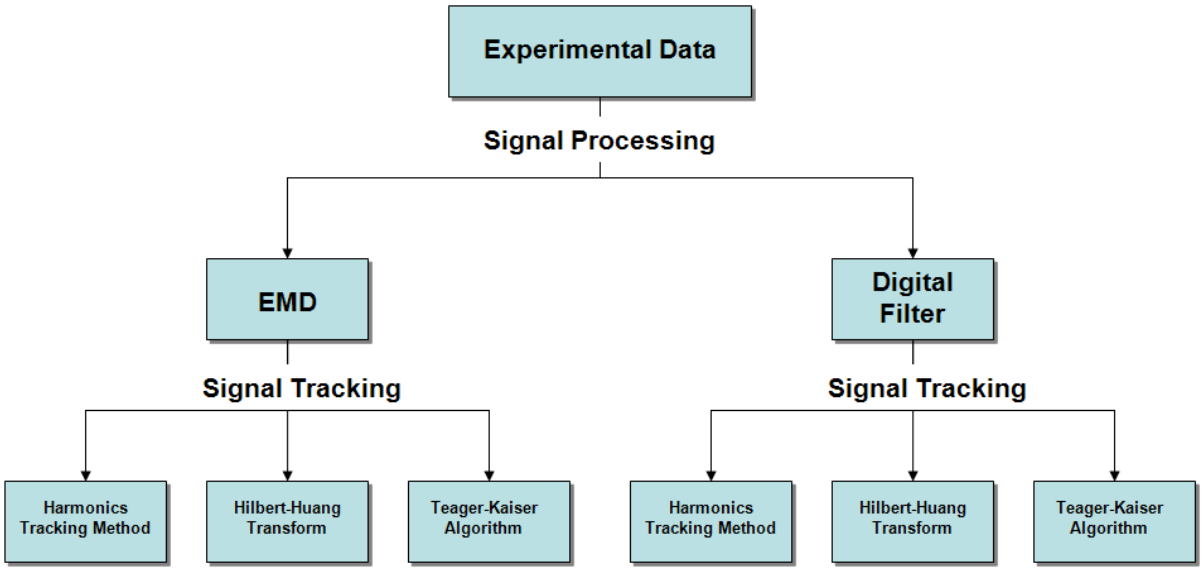

Figure 5.1. Data processing flow chart

5.1 Horizontal Long Beam Data Processing Results

From the experiment involving the horizontal long beam, the velocity profile was collected and mode one vibration was extracted by using either EMD or the 4^{th} order low pass filter. This data was then used to calculate the instantaneous amplitudes and frequencies using the HTM. Figure 5.2 shows the results when using the digital filter then HTM while Fig. 5.3 is the results after using the EMD then HTM.

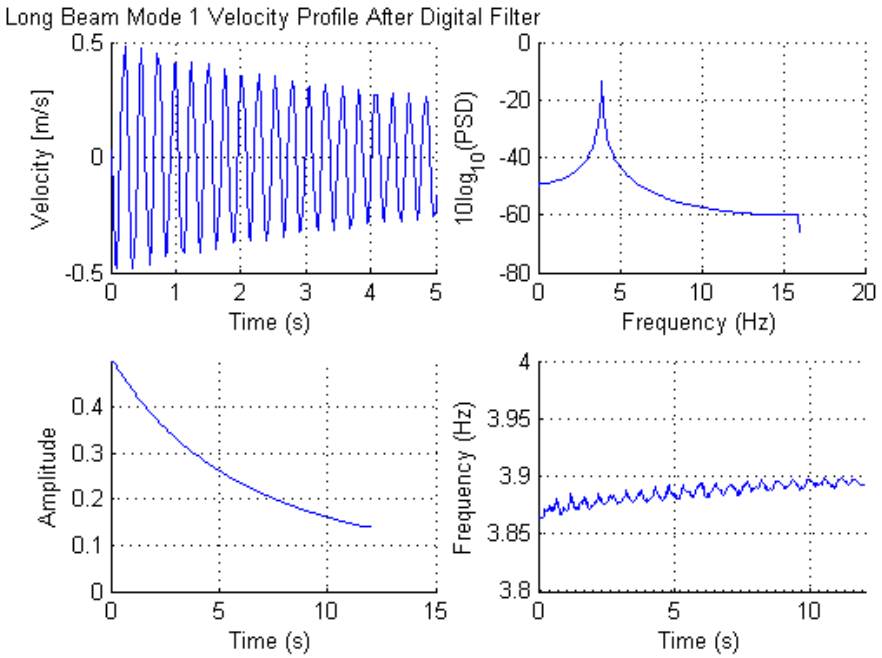

Figure 5.2. HTM results from long beam data after low pass digital filter.

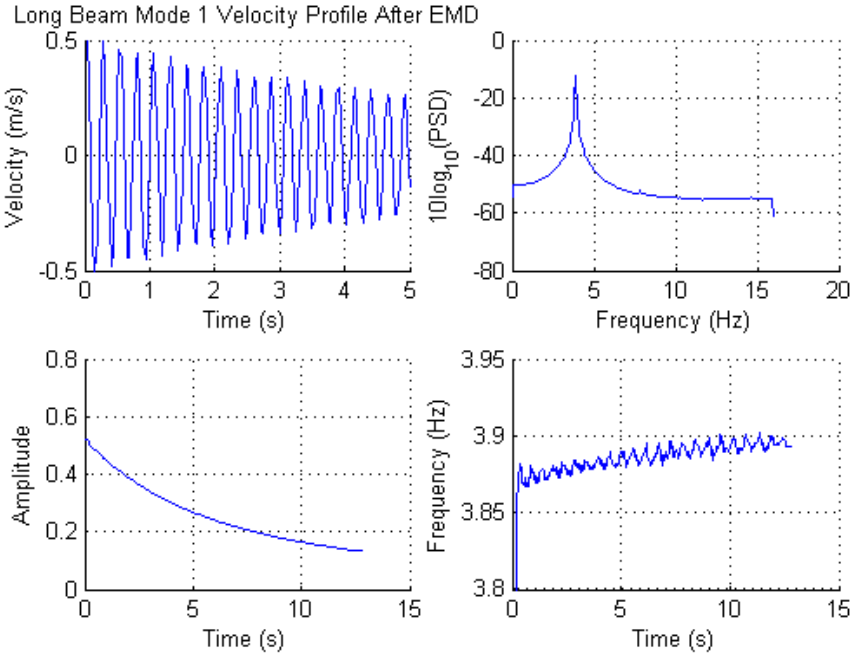

Figure 5.3. HTM results from long beam data after EMD.

The Hilbert-Huang transfer was also used to determine the instantaneous amplitude and frequency of the extracted mode one from the horizontal long beam

data. Figure 5.4 displays the HHT results after using the digital filter while Fig. 5.5 is the results after using the EMD then HHT.

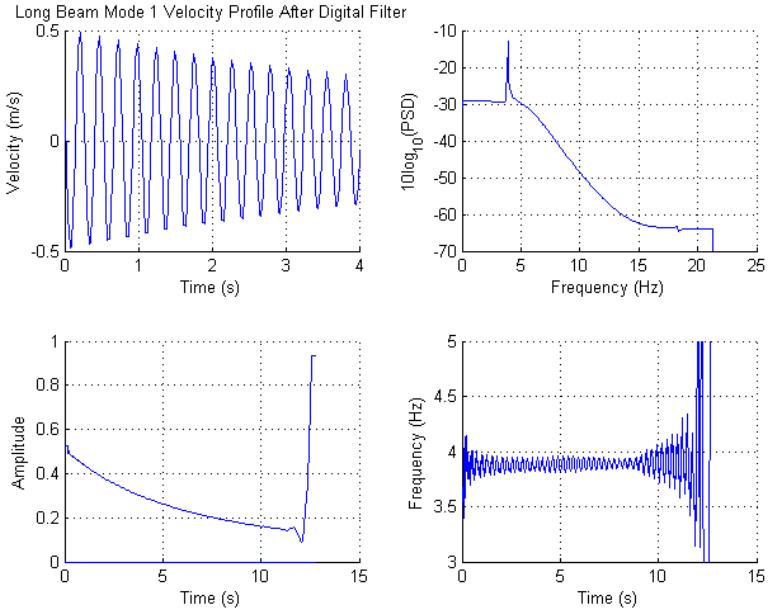

Figure 5.4. HHT results from long beam data after low pass digital filter.

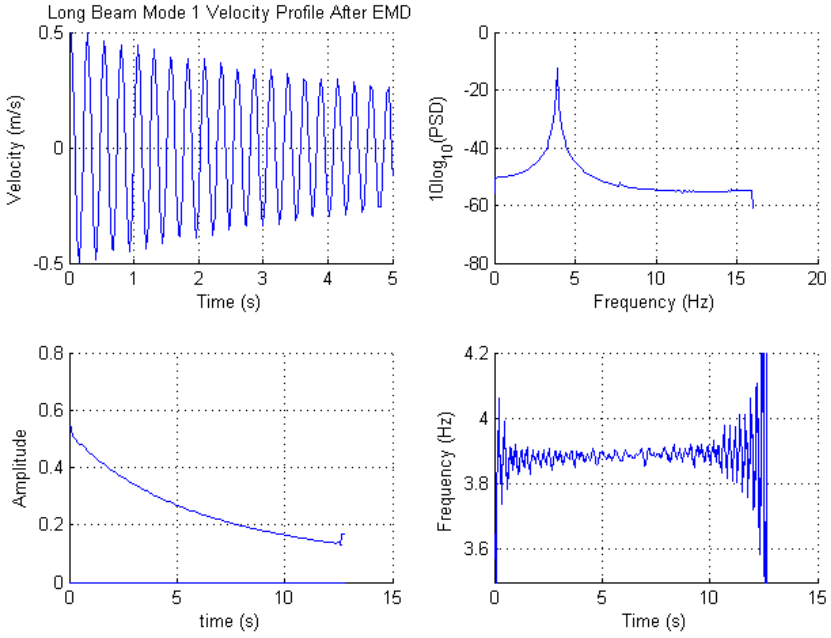

Figure 5.5. HHT results from long beam data after EMD.

Again from the velocity profile collected from the horizontal long beam, mode one vibration was extracted by using EMD or the 4th order low pass filter. This data was then used to calculate the instantaneous amplitudes and frequencies using TKA. Figures 5.6 show the TKA results when using the digital filter while Fig. 5.7 displays TKA processing results after using EMD.

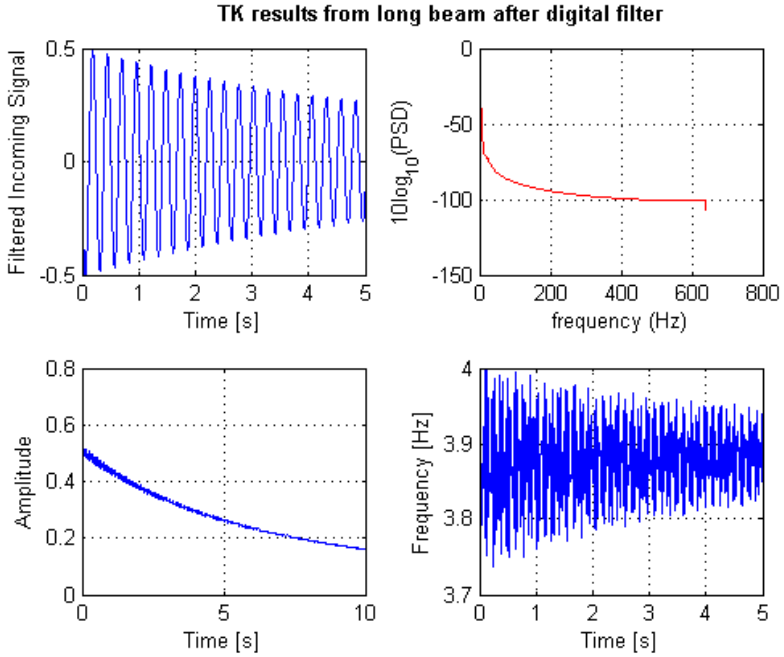

Figure 5.6. TKA results from long beam after digital filter.

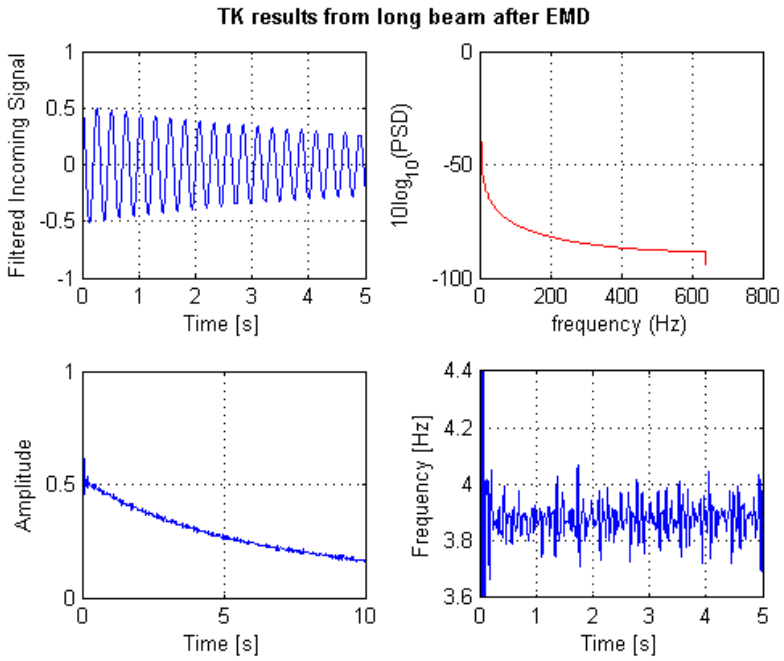

Figure 5.7. TKA results from long beam after EMD.

By comparing the signal tracking results from Figs. 5.2 – 5.7 it becomes clear that HTM is superior to both HHT and TKA; particularly with regards to instantaneous frequency calculations. As with the example from section 4.4, TKA shows far too little resolution to provide valuable frequency data. The outcome of signal tracking with HHT is again dominated by large edge effects which distort the most valuable instantaneous frequency data. Conversely, HTM provides superior frequency and amplitude tracking data. There is little to no Gibbs Phenomenon when using HTM and the resolution is precise enough to reveal the nonlinear frequency and amplitude relationship. It also becomes apparent that both signal processing methods, used to extract mode one vibration, yield sufficient and consistent data for further signal tracking by HTM. However, the nonlinearity within the instantaneous frequency is more pronounced when using EMD. Figure 5.8 gives a graphical representation of the effective signal

processing and tracking algorithms. When analyzing the data from the two additional experiments concerning the horizontal short beam and the vertical long beam, the same algorithm has been used. However, because the outcomes of these are similar to those previously shown, only the results from signal tracking with HTM will be displayed.

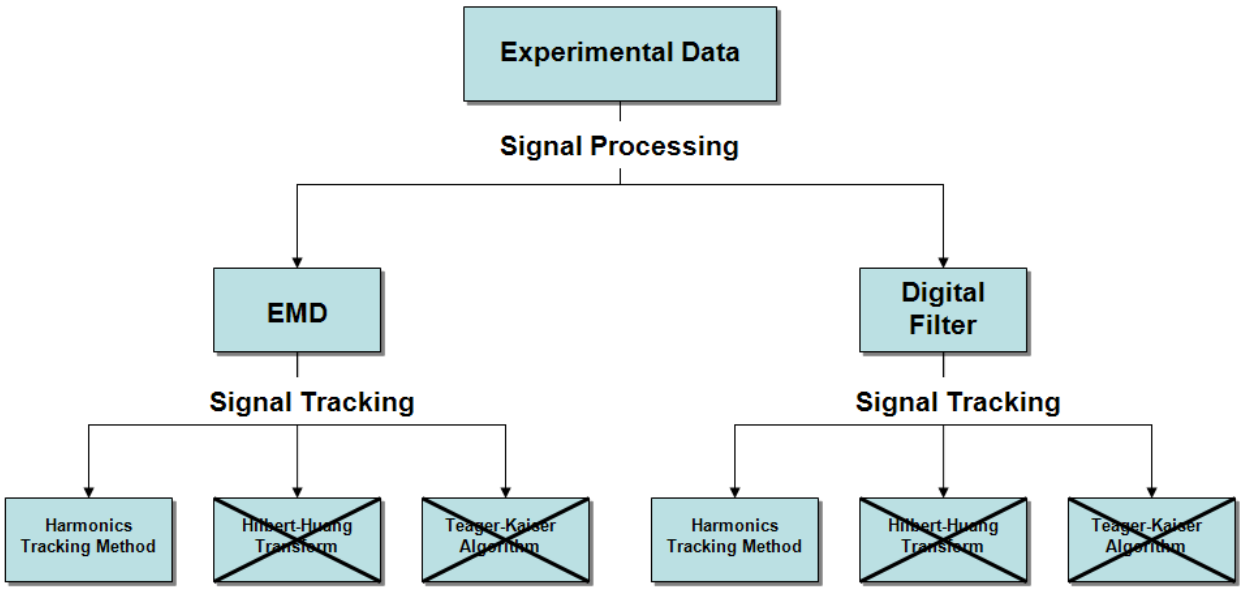

Figure 5.8. Flowchart of effective algorithms

5.2 Horizontal Short Beam Data Processing Results

As with the previous section, the velocity profile of the horizontal short beam has been collected and analyzed. Mode one vibration has been isolated using either the low pass digital filter or EMD. The results have been further analyzed using all three signal tracking techniques, HTM, HHT, and TKA. Similar to processing the horizontal long beam data, both HHT and TKA fail to proved accurate instantaneous frequency calculations without large distortions. For brevity, only the outcome of HTM in

combination with EMD or the low pass filter will be shown within this work. Figure 5.9 presents HTM signal tracking results after using the 4th order digital filter while Fig. 5.10 shows the HTM analysis after using EMD.

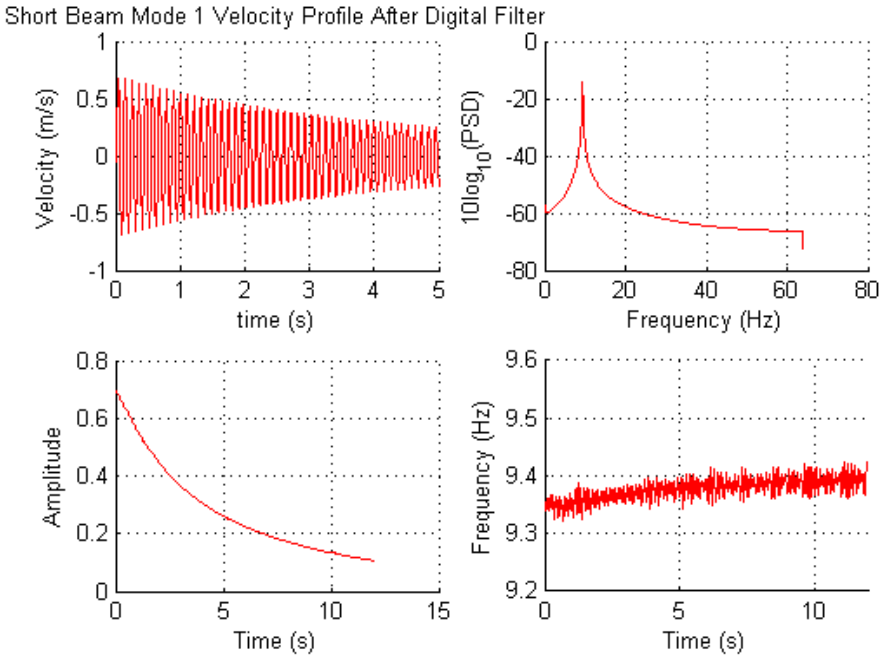

Figure 5.9. HTM results from short beam data after low pass digital filter.

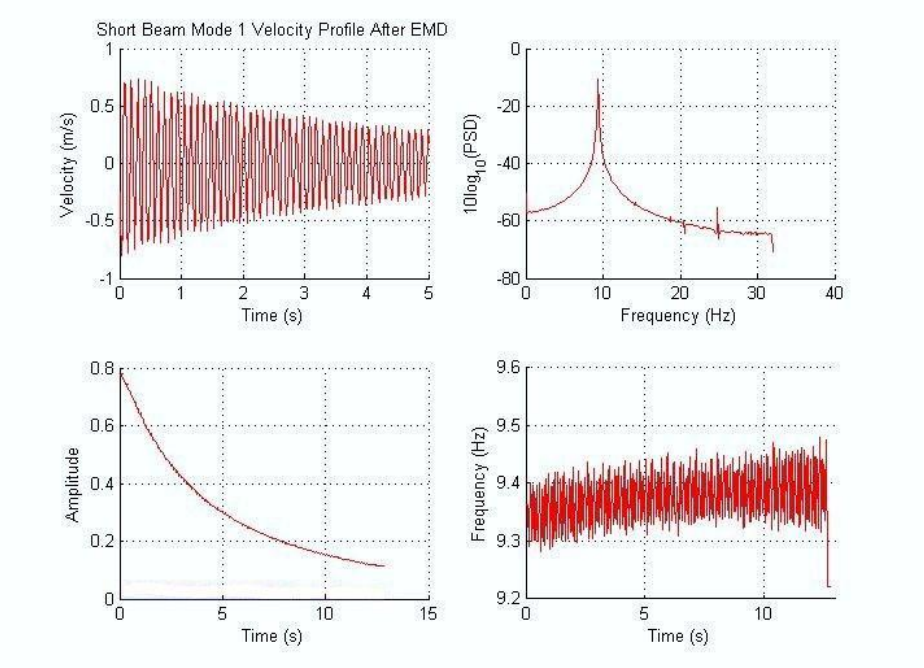

Figure 5.10. HTM results from short beam data after EMD.

From both of these figures, the limits of this type of analysis can be seen. With respect to the response of the short beam, it has a higher oscillating frequency and dampening occurs much faster than with the longer beam. The sharp frequency and amplitude change make precision signal tracking more difficult. The results have less resolution that those seen from the longer cantilever beam. However, HTM proves again to be much superior to both HHT and TKA. Interestingly, here is it seems that the digital filter in combination with HTM provides clearer data that when combined with EMD, which is in contrast to the results in section 5.1.

5.3 Vertical Long Beam Data Processing Results

Similarly to the horizontal beams, the experimental data from the vertical beam will be subjected to the same type and algorithmic analysis. Outcomes from signal tracking with HHT and TKA will not be shown since they yield little to no useful instantaneous frequency data. These results are similar to those found in section 5.1. Figures 5.11 – 5.12 present the HTM signal tracking analysis results from the data involving the vertical beam experiment when coupled with either the 4^{th} order low pass digital filter or EMD.

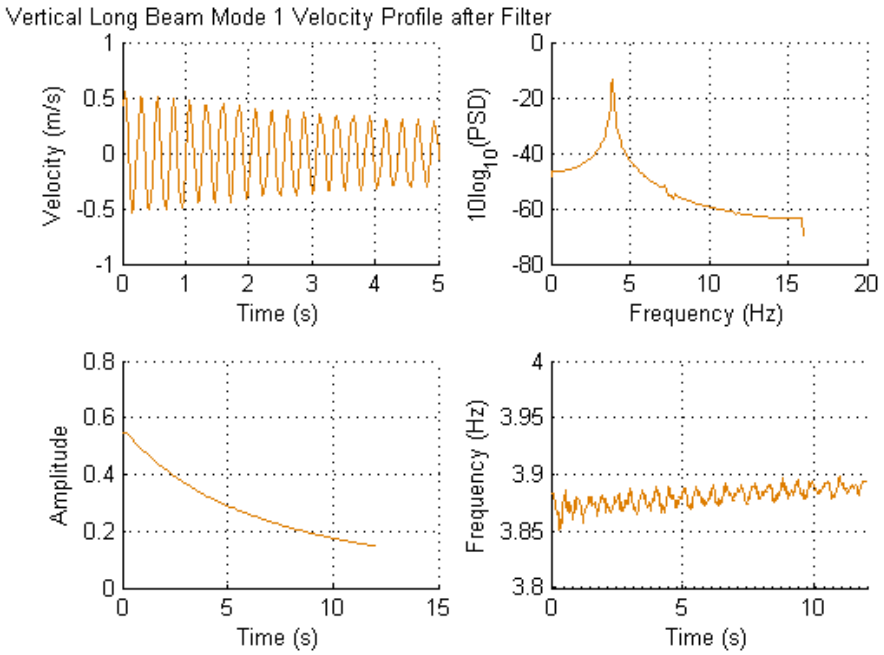

Figure 5.11. Vertical beam HTM results after digital filter

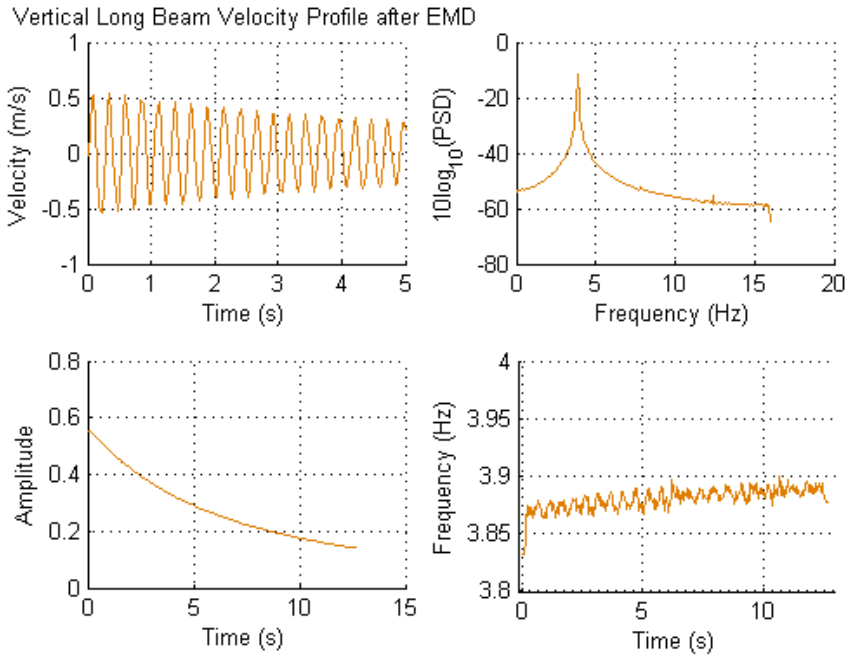

Figure 5.12. Vertical beam HTM results after EMD

Initial examination of these HTM signal tracking results indicate that they are very similar to those found in Figs. 5.2 and 5.3. This is as expected as the beam is

identical to that used in section 5.1; however it is placed in the vertical orientation as opposed to horizontally positioned.

Chapter 6 – Interpreting Results

Throughout the previous chapters, an alternative method of collecting data for the determination of nonlinearity of vibrating structures had been introduced. This method makes use of transient and free vibrations as opposed to forced steady-state responses. Once data has been collected it must be processed to isolate the particular mode of interest, in this case mode one. Either a Butterworth low pass digital filter or EMD has been used for this. The next step is to use signal tracking techniques to calculate the instantaneous frequency and amplitude of the incoming signal. Within this work, either HTM, HHT, or TKA have been used for these calculations. Once this data is gathered, is it desired to find the nonlinear relationship between instantaneous amplitude and frequency. From this correlation, a determination of nonlinear softening or hardening and the strength of nonlinearity can be made.

Within chapter six, the amplitude versus frequency data seen from chapter five will be presented. By visually examining the plots and through least squares fits of this data, nonlinear characteristics will be found. Section 6.2 will address further data processing considerations when using TKA for signal tracking.

6.1 Interpreting Results

By comparing the previous sets of results within sections 5.1 – 5.3, it becomes clear that both HHT and TKA fail to provide accurate data with respect to the instantaneous frequency of the signal. The Hilbert-Huang transfer either distorts this data with large Gibbs phenomenon effects, or is not sensitive enough to pick up the

nonlinearity within the signal. The Teager-Kaiser algorithm has also shown to be inadequate in extracting the instantaneous frequency for this type of analysis. The harmonics tracking method however, gives superior data when compared to HHT and TKA. Furthermore, HTM provides useful and comparable data when coupled with either EMD or the low pass digital filter.

For this work the nonlinearity within the instantaneous amplitude versus frequency is of interest. Thus, plots of the amplitude versus frequency of each useful algorithm, seen in Fig. 5.8, have been made and can be seen in Figs. 6.1 – 6.6. In addition, each of these data sets have been least-squares fitted with a second order polynomial.

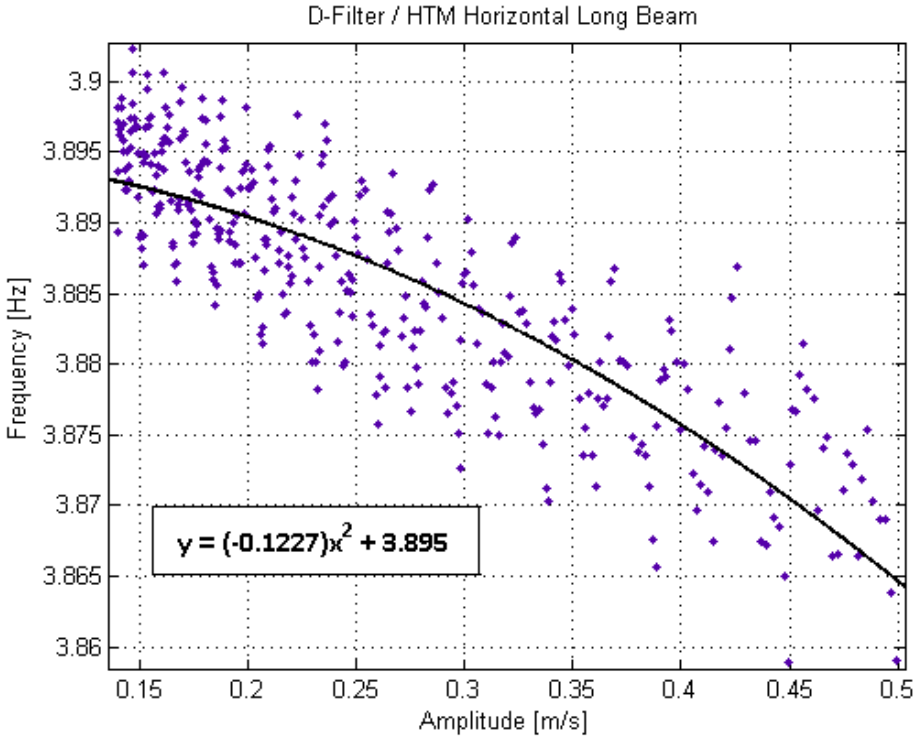

Figure 6.1. Amplitude vs. Frequency – Digital Filter/HTM long beam

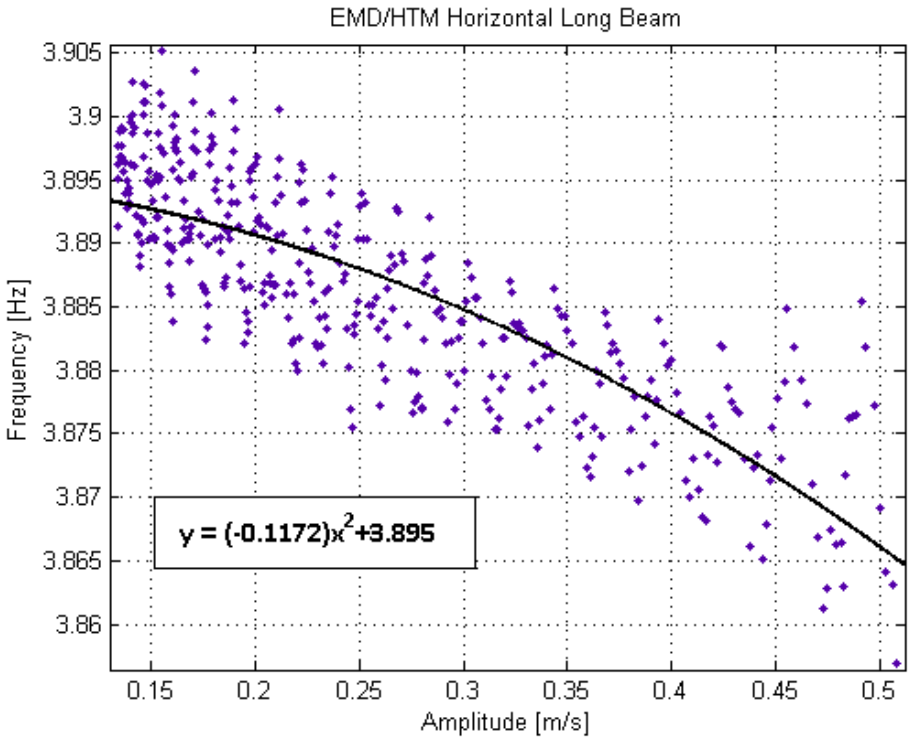

Figure 6.2. Amplitude vs. Frequency – EMD/HTM long beam

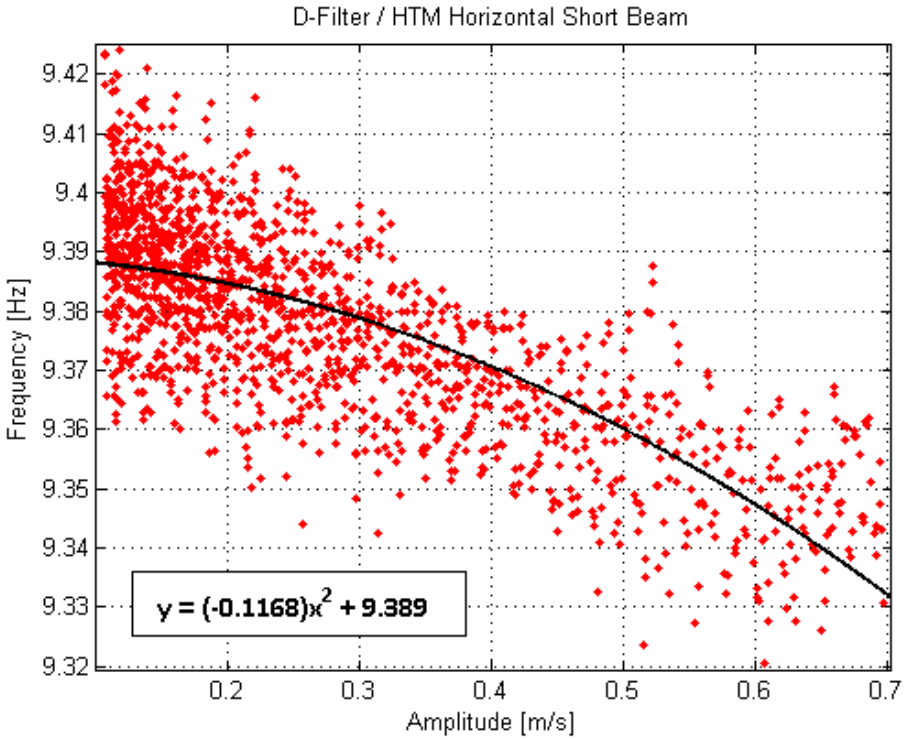

Figure 6.3. Amplitude vs. Frequency – Digital Filter/HTM short beam

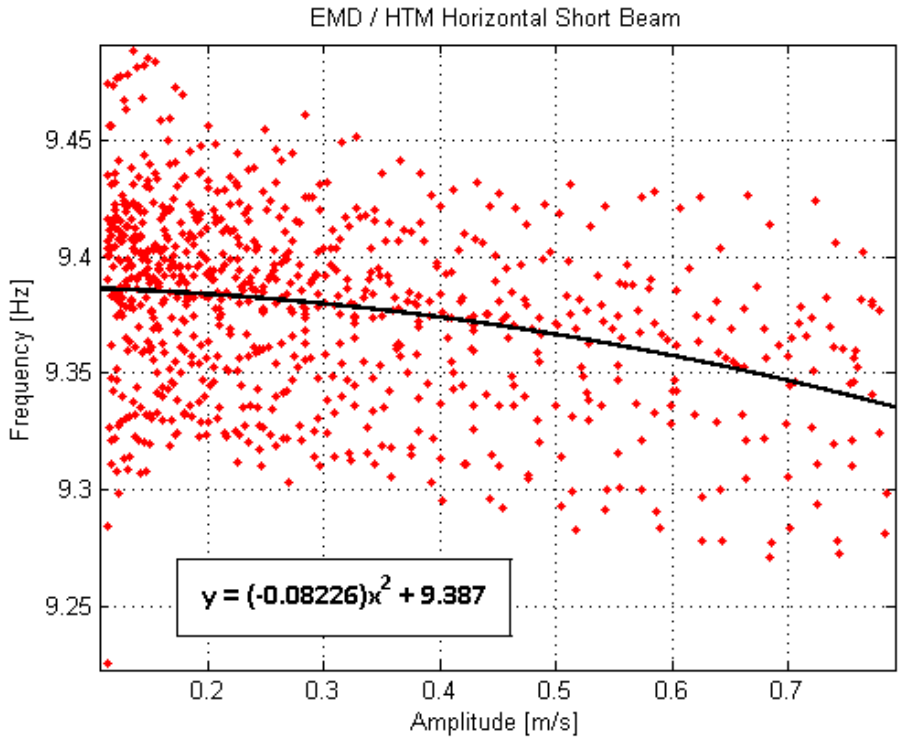

Figure 6.4. Amplitude vs. Frequency – EMD/HTM short beam

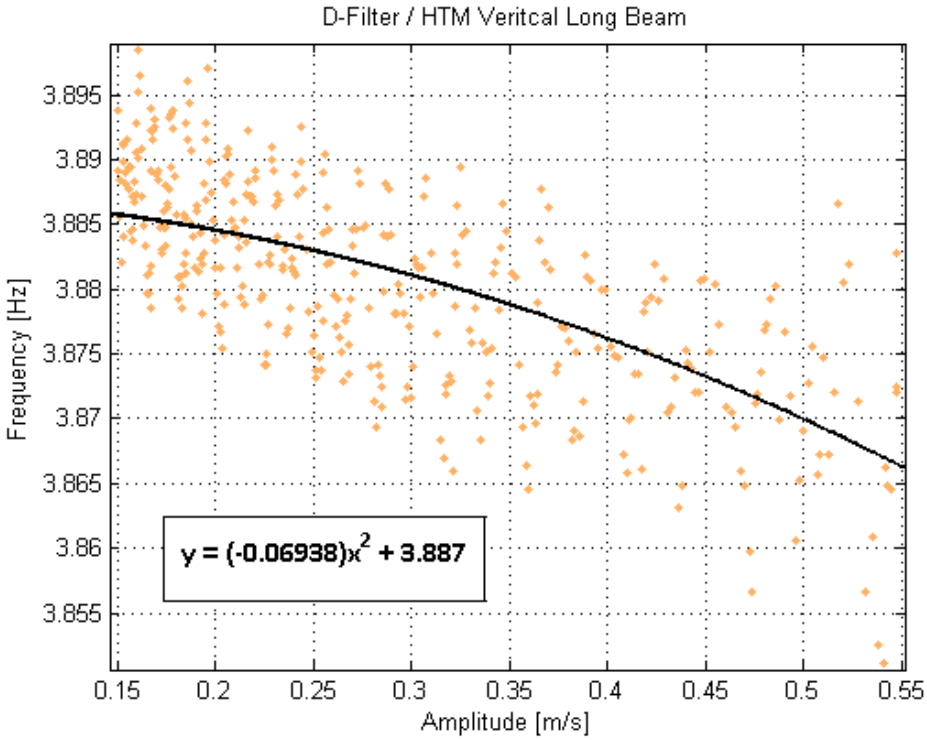

Figure 6.5. Amplitude vs. Frequency – Digital Filter/HTM vertical beam

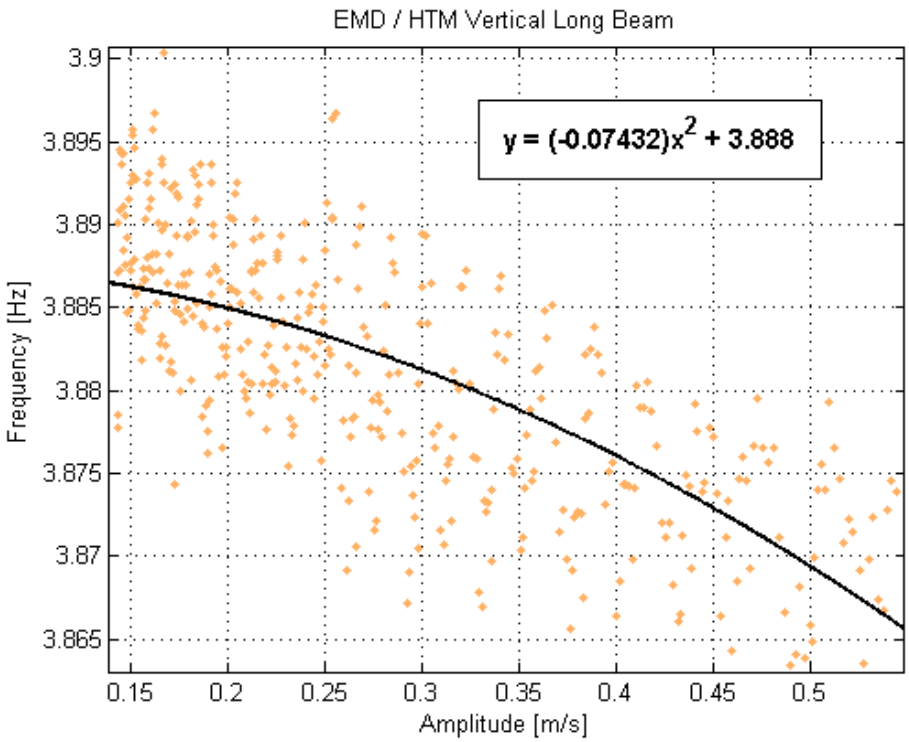

Figure 6.6. Amplitude vs. Frequency – EMD/HTM vertical beam

The data found in Figs. 6.1 – 6.6 have been least-squares fitted to a second order polynomial of the form found in Eq. 6.1. Here ω, A, ω_0, and λ correspond to frequency, amplitude, initial frequency value, and the constant nonlinear coefficient respectively. A negative λ value would result in a downward sloping trend in instantaneous frequency versus amplitude plot which would indicate a softening effect. An upward trend from a positive λ value would indicate hardening, as shown in Fig. 6.7.

$$\omega = \lambda A^2 + \omega_0 \tag{6.1}$$

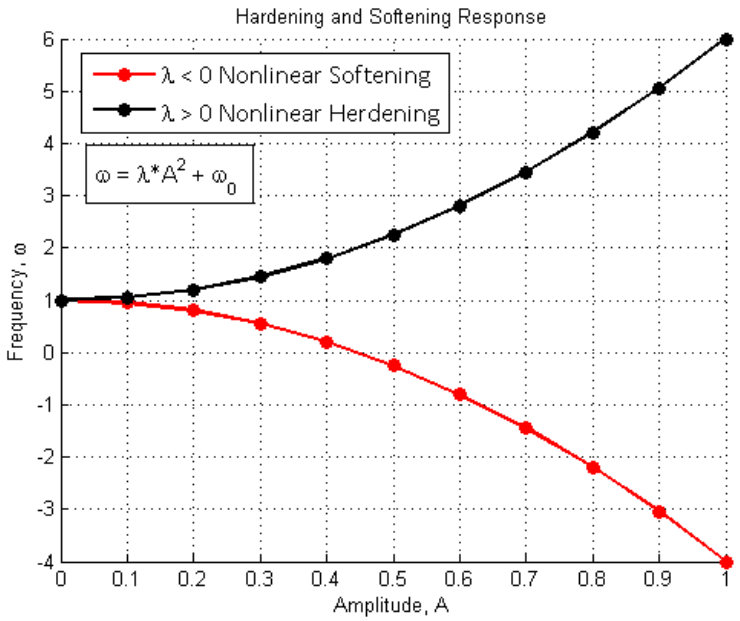

Figure 6.7 Example of nonlinear hardening and softening response

Tables 6.1 – 6.3 provide the least square fit values for each data set along with the 95% confidence bounds values within the parentheses. Additionally, the coefficient of determination, r^2, for each least-squares fit have also been provided. This value signifies the "*goodness*" of the fit, with a value of *1* corresponding to a perfect fit. This coefficient has been calculated using Eq. (6.2). Within this equation, S_t is the total sum of the residuals between the original data points and the mean. The sum of the squares of the residuals around the least-squares fit is represented by the variable S_r. S_t and S_r are calculated using Eqs. (6.3) and (6.4) respectively.

$$r^2 = \frac{S_t - S_r}{S_t} \tag{6.2}$$

$$S_t = \sum_{i=1}^{i=n} \left(\omega_i - \overline{\omega}\right)^2 \tag{6.3}$$

$$S_r = \sum_{i=1}^{n} \left(\omega_{i,DATA} - \omega_{i,FIT}\right)^2 = \sum_{i=1}^{n} \left(\omega_{i,DATA} - \lambda A_i^{\,2} - \omega_0\right) \tag{6.4}$$

Table 6.1. Horizontal long beam least-squares fit data.

	Horizontal Long Beam	
	EMD/HTM	D-Filter/HTM
λ	-0.1172 (-0.1253, -0.1092)	-0.1227 (-0.1303, -0.115)
ω_0	3.895 (3.895, 3.896)	3.895 (3.895, 3.896)
r^2	0.6705	0.7209

Table 6.2. Horizontal short beam least-squares fit data.

	Horizontal Short Beam	
	EMD/HTM	D-Filter/HTM
λ	-0.08226 (-0.1009, 0.06359)	-0.1168 (-0.1221, -0.1115)
ω_0	9.387 (9.384, 9.391)	9.389 (9.389, 9.39)
r^2	0.08382	0.5495

Table 6.3. Vertical long beam least-squares fit data.

	Vertical Long Beam	
	EMD/HTM	D-Filter/HTM
λ	-0.07432 (-0.08172, -0.06691)	-0.06938 (-0.07742, -0.06134)
ω_0	3.888 (3.887, 3.889)	3.887 (3.886,3.888)
r^2	0.4948	0.4298

From these results it can be concluded that the long, short, and vertical cantilever beams all exhibit a softening effect within mode one vibration. In other words, the frequency increases as the amplitude decreases. This relationship between frequency and amplitude is seen to be slightly nonlinear in all cases through the value of the nonlinear coefficient, λ, of the fitted polynomial. The negative value of this

coefficient indicates softening as opposed to a positive value which would indicate hardening. These findings are in contrast with results from [7], which predict and show a nonlinear hardening effect within mode one vibration.

Three experiments were run which involved two horizontal beams of different lengths, and a vertically positioned beam. All three experimental results showed a softening effect, whether using the low pass filter or EMD for signal processing. However, the magnitude of the nonlinear coefficient for each experiment changes depending on the length of the beam and its orientation. This coefficient takes on a significantly smaller magnitude for the vertical orientation when compared to the results using the same beam but in the horizontal position. It becomes approximately 60% of the value in the horizontal case. A change in this direction is expected due to gravitational forces acting upon the vertically oriented beam. As the beam vibrates horizontally, the gravitational force would be pulling downward on the tip of the beam. Thus, gravity would be acting to encourage larger amplitude displacements through time. Figure 6.8 gives a visual representation.

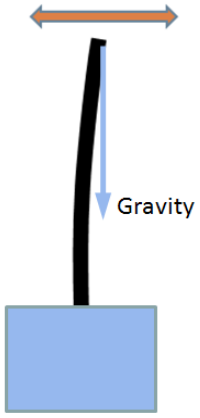

Figure 6.8. Sketch of vertical beam with gravitation force acting

This ultimately leads to a hardening effect on the nonlinear relationship between amplitude and frequency. Thus, the magnitude of the nonlinear coefficient becomes smaller.

To investigate this further and provide a clear illustration of how gravitational effects cause a hardening effect, consider the pendulum-spring system seen in Figs. 6.9 – 6.10. Here the string of the pendulum will be considered massless.

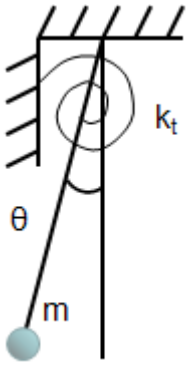

Figure 6.9. Downward hanging pendulum with spring

For this system the kinetic energy, *T*, and the potential energy, *P*, are:

$$T = \frac{1}{2} m\left(l\dot{\theta}\right)^2 \tag{6.5}$$

$$V = \frac{1}{2} k_t \theta^2 - mgl\cos\left(\theta\right) \tag{6.6}$$

Here m, l, k_t, and θ represent the pendulum mass, pendulum length, total spring stiffness, and angular displacement respectively.

As derived within [3], the equation of motion for the downward hanging system takes the form in Eq. (6.7). The gravitational term within Eq. (6.6) takes a negative value, which intern gives a negative value to the cubic term within Eq. (6.7). The

negative value of this coefficient correlates to nonlinear softening. Here, it can be seen how gravity is acting to enforce softening.

$$\ddot{\theta} + \left[\left(\frac{k_t}{mL^2} + \frac{g}{L} \right) - \frac{g}{6L} \theta^2 \right] \theta = 0 \tag{6.7}$$

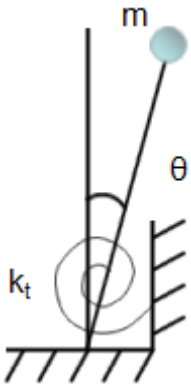

Figure 6.10. Upward hanging pendulum with spring

An example which is more analogous to the vertically oriented vibrating beam would be that seen in Fig. 6.9. For this upward pendulum-spring system the kinetic energy and the potential energy are described as below.

$$T = \frac{1}{2} m \left(l \dot{\theta} \right)^2 \tag{6.8}$$

$$V = \frac{1}{2} k_t \theta^2 + mgl \cos(\theta) \tag{6.9}$$

The corresponding equation of motion then becomes:

$$\ddot{\theta} + \left[\left(\frac{k_t}{mL^2} - \frac{g}{L} \right) + \frac{g}{6L} \theta^2 \right] \theta = 0 \tag{6.10}$$

Here the gravitational term and thus the cubic nonlinear coefficient take on a positive value, which indicates nonlinear hardening. For this scenario, the gravitational force is directly contributing to a hardening effect. This is also the case for the vertically

oriented cantilever beam. Gravity acting upon the beam causes hardening within the nonlinear coefficient. However, it is not strong enough to cause complete hardening. Rather it weakens the softening effect, which intern lowers the magnitude of the nonlinear coefficient causing a positive shift in value. This can be seen through Tables 6.1, 6.3, and later Tables 6.4 and 6.6.

6.2 Additional Signal Processing Considerations

In the previous two chapters it has been shown how TKA fails to provide useful data when used with either the low pass digital filter or EMD. However, upon further investigation it has been found that TKA can yield significantly improved signal tracking results when coupled with the correct combination of signal processing techniques. The two combinations include EMD followed by the digital filter, or the digital filter followed by an additional digital filter.

The low pass digital filter acts as a transfer function which intensifies the frequencies below the set cutoff frequency, and diminishes those above. Thus, when the incoming signal is fed through the filter multiple times, it works to extract mode one more efficiently every time. This provides clearer data for TKA to analyze, which in turn is significantly more accurate in signal tracking. The disadvantage to this algorithm is that the digital filter will produce a phase shift within the filtered data, and any additional filtering will increase this shift.

This process works to improve the TKA results, however does little to no improvement for HTM and HHT. Additional filtering will also not improve the quality of results for any data from the experiment involving the short cantilever beam; therefore

only the additional TKA results from the horizontal and vertical long beam will be discussed here. Figures 6.11 – 6.14 display the TKA results from the horizontal long beam, while Figs. 6.15 – 6.18 are from the experiment involving the beam which was vertically positioned.

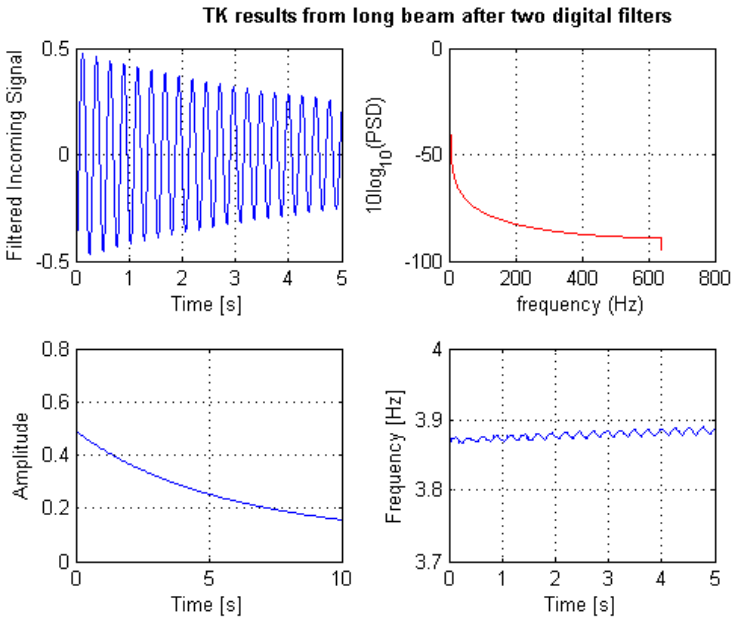

Figure 6.11. Horizontal Long Beam TKA analysis after two digital filters

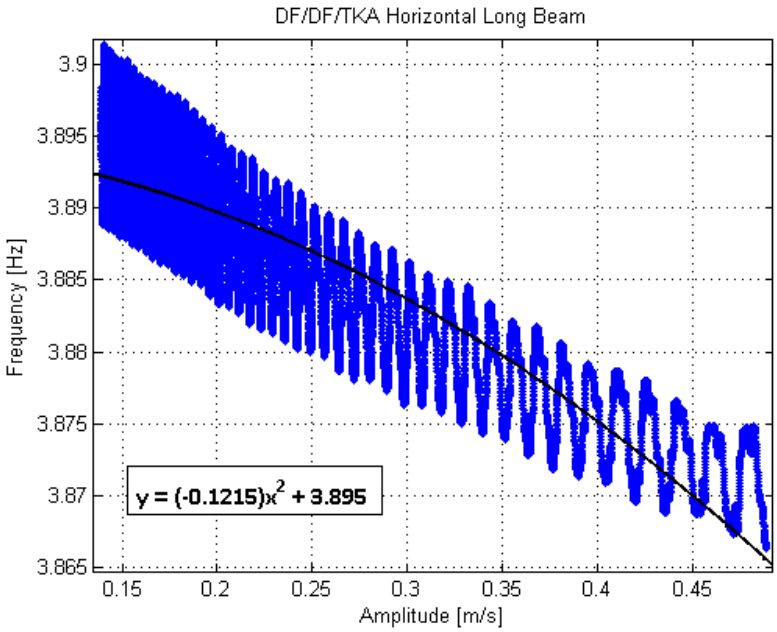

Figure 6.12. Amplitude vs. Frequency – DF/DF/TKA Horizontal long beam

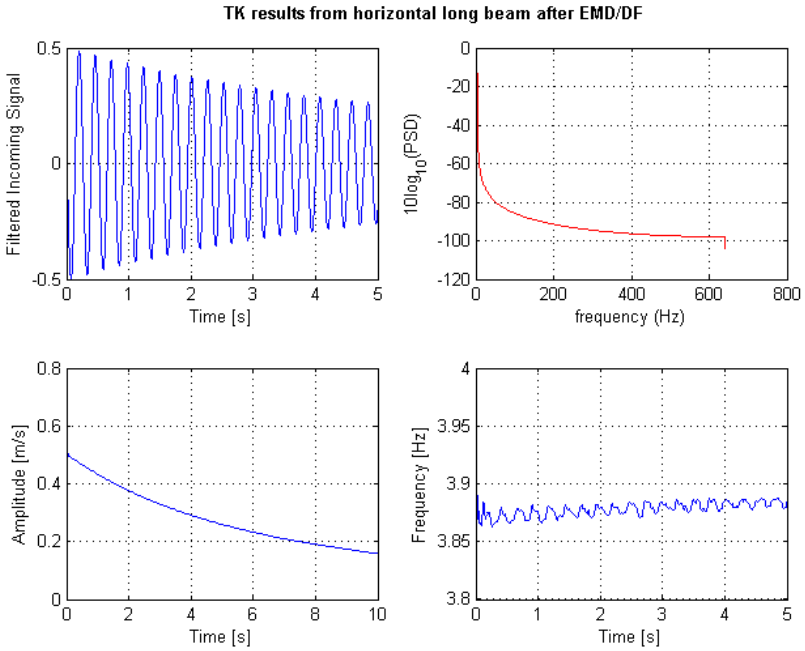

Figure 6.13. Horizontal Long Beam TKA analysis after EMD and digital filter

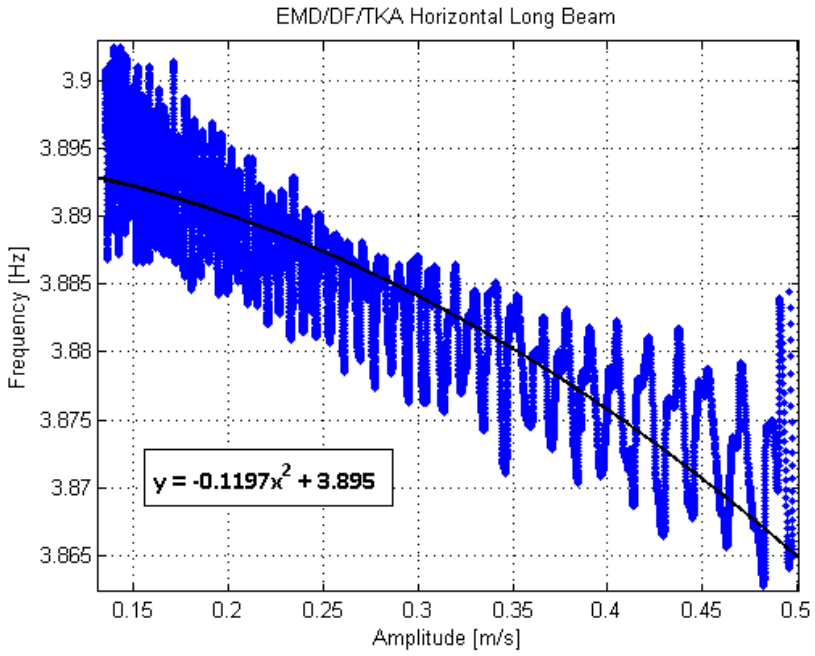

Figure 6.14. Amplitude vs. Frequency – EMD/DF/TKA Horizontal long beam

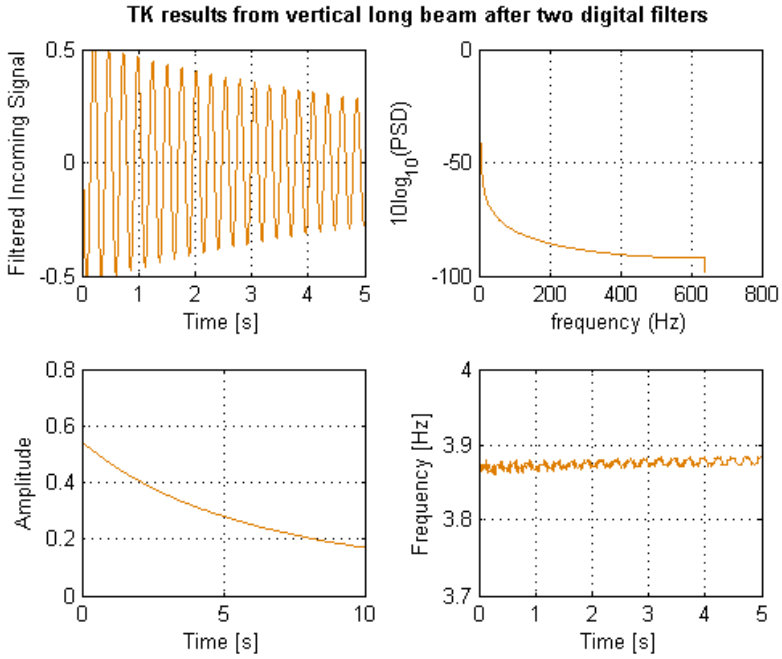

Figure 6.15. Vertical Long Beam TKA analysis after two digital filters

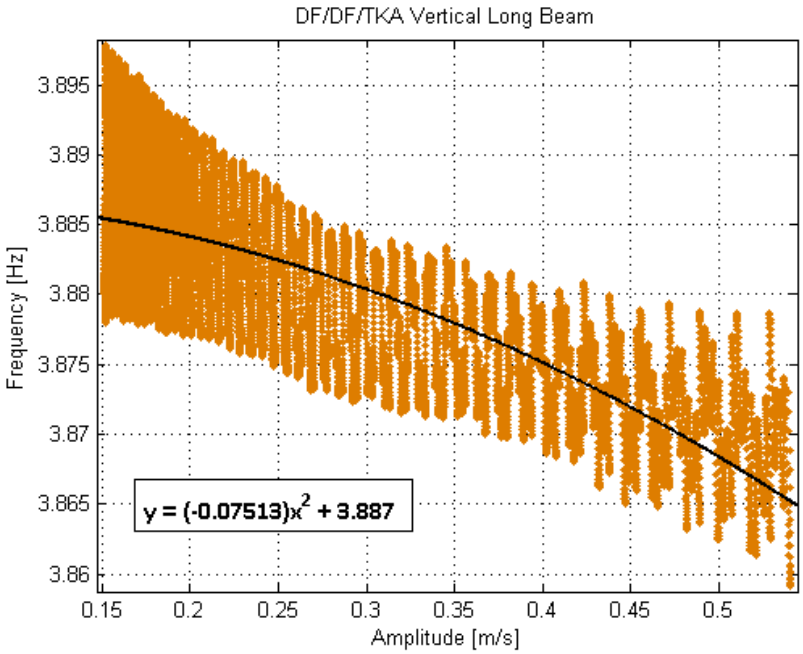

Figure 6.16. Amplitude vs. Frequency – DF/DF/TKA Vertical long beam

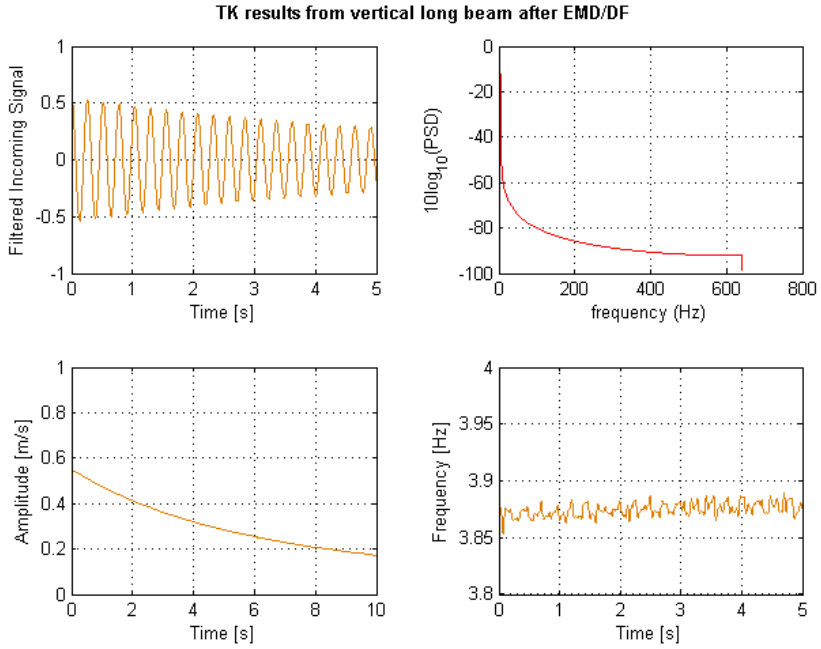

Figure 6.17. Vertical Long Beam TKA analysis after EMD and digital filter

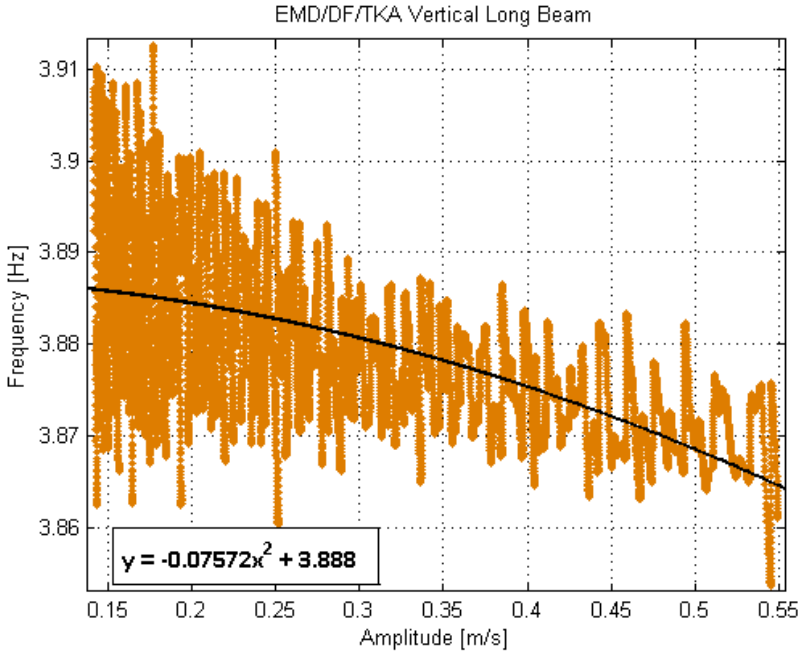

Figure 6.18. Amplitude vs. Frequency – EMD/DF/TKA Vertical long beam

These additional results also show a softening effect within the amplitude versus frequency relationship; however the nonlinearity is not as clearly defined through visual

examination of the plots. Comparing these findings with the outcomes in previous sections leads to very similar conclusions. The least-squares fit also produces coinciding coefficients which can be seen in the plots above or in Tables 6.4 and 6.6 for comparison.

Table 6.4 All horizontal long beam least-squares fit results

	Horizontal Long Beam				
	EMD/HTM	D-Filter/HTM	D-Filter/D-Filter/TKA	EMD/D-Filter/TKA	Average
λ	-0.1172 (-0.1253, -0.1092)	-0.1227 (-0.1303, -0.115)	-0.1215 (-0.1227, -0.1203)	-0.1197 (-0.1209, -0.1186)	-0.120275
ω_0	3.895 (3.895, 3.896)	3.895 (3.895, 3.896)	3.895 (3.894, 3.895)	3.895 (3.895, 3.895)	3.895
r^2	0.6705	0.7209	0.7415	0.741	0.718475

Table 6.5 All horizontal short beam least-squares fit results

	Horizontal Short Beam		
	EMD/HTM	D-Filter/HTM	Average
λ	-0.08226 (-0.1009, 0.06359)	-0.1168 (-0.1221, -0.1115)	-0.09953
ω_0	9.387 (9.384, 9.391)	9.389 (9.389, 9.39)	9.388
r^2	0.08382	0.5495	0.31666

Table 6.6 All vertical long beam least-squares fit results

	Vertical Long Beam				
	EMD/HTM	D-Filter/HTM	D-Filter/D-Filter/TKA	EMD/D-Filter/TKA	Average
λ	-0.07432 (-0.08172, -0.06691)	-0.06938 (-0.07742, -0.06134)	-0.07513 (-0.07634, -0.07392)	-0.07572 (-0.07743, -0.074)	-0.073638
ω_0	3.888 (3.887, 3.889)	3.887 (3.886,3.888)	3.887 (3.887,3.887)	3.887 (3.887,3.888)	3.88725
r^2	0.4948	0.4298	0.5051	0.323	0.438175

Although, through the use of additional filtering, TKA can yield significantly improved results, the use of the filter causes an additional phase shift. Also,

the use of an additional filter creates more distorted data near the beginning of the incoming signal which must be ignored. Furthermore, the least squares fit of the 2nd order polynomial appears to not fit the amplitude versus frequency plot as well. Although still softening, this relationship becomes more linear in nature.

Chapter 7 – Conclusion and Recommendations

7.1 Conclusion

Within this work an alternate method for determining nonlinearity of a structure has been proposed. This method makes use of free transient vibrations as opposed to analyzing forced steady state responses. In order to investigate the effectiveness of this method, a cantilever beam has been subjected to vibratory analysis. Although simple, a cantilever beam is used in various applications, including advanced MEMS devices. Moreover, the slight nonlinearity of a cantilever beam has proven in previous works to be difficult to characterize and often contradicts with theory.

An advanced signal processing technique known as the Harmonics Tracking Method has been utilized to perform instantaneous amplitude and frequency analysis. Additionally, HTM has been compared to two other more traditional signal tracking methods, the Teager-Kaiser Algorithm and the Hilbert-Huang Transform. Furthermore, two signal processing techniques, a 4^{th} order low pass digital filter and the empirical mode decomposition were applied to the experimental data in order to isolate the most essential information. The results of which have all been compared.

The results of the experiment clearly show that numerous modes of vibration exist. The frequency domain plots also confirm this assessment. Both techniques used to extract mode one vibration have proven successful. However, as noted before, there is a phase shift when using the low pass filter. Also, since the data has been fed through the filter backwards, the end of the data is distorted and thus has been ignored in further analysis.

Once mode one has been extracted, all three signal tracking methods were used to calculate the instantaneous frequency and amplitude of the signal. Examining these results leads to the conclusion that HTM is significantly more accurate than both TKA and HHT with regards to this type of signal. TKA has far too little resolution to be used within this application when computing instantaneous frequency. HHT, although more powerful than TKA, also has too little resolution to be capable of picking up the nonlinearity within the instantaneous amplitude. Furthermore, large edge effects known as the Gibbs phenomenon distort the beginning and end of the instantaneous frequency data, which renders the data virtually useless for determining nonlinearity. In contrast, HTM provides the clearest data with little to no edge effects. The resolution that HTM provides is also significantly superior to both TKA and HHT, thus providing the best data for nonlinearity determination. With regards to the signal processing methods, EMD and the low pass filter, both provide enough consistency within the data for HTM to generate nearly identical results. Therefore, both methods can be used in conjunction with HTM to produce accurate data. However, because of the small phase shift and distortions associated with the low pass filter, it is recommended that EMD be used for best results.

Using the results from HTM analysis, plots of the instantaneous amplitude versus frequency of the signals were created. A second order polynomial of the form in Eq. (6.1) has been fitted to this data using a least-squares method. From this equation, the value of the nonlinear coefficient in all of the data sets can be seen to take a negative value. From this, and by visually examining the data, the nonlinearity of the cantilever

beam can be characterized as softening. The experimental results from the long cantilever beam in the vertical position yields some interesting results. For this experiment, the nonlinear coefficient takes a more positive value indicating that gravity plays a role in the response of the beam. Within this orientation, gravity creates a hardening effect which lowers the magnitude of the nonlinear coefficient. This result agrees with the pendulum-spring example given in section 6.1; which predicts gravity has yielding a hardening effect.

Two additional signal processing algorithms were also examined and have been shown to significantly improve the performance of TKA. These two additional algorithms involve processing the data twice; through the combination of EMD followed by the digital filter, or the digital filter followed by an additional digital filter. Using these techniques, the TKA analysis yields much more accurate data, which coincides with the original HTM results. Least-square fits of the frequency versus amplitude relationship yields nearly identical coefficients, which can be seen in Tables 6.4 and 6.6.

Although additional signal processing can improve the outcome of TKA, it has little effect on HTM and HHT. HTM will still produce consistent and accurate data while HHT has large Gibbs phenomenon effects. Using additional digital filtering can improve the quality of data produced from TKA analysis, however with each additional filter comes another phase shift and additional edge effects which must be ignored. Also, when inspecting the amplitude versus frequency relationships, seen within Figs. 6.12, 6.14, 6.16, and 6.18, the nonlinearity cannot clearly be seen. Although still classified as softening, a more linear relationship emerges, which is in contrast to the HTM results.

Although TKA, when used in combination with additional signal processing, yields significantly improved results that coincide with HTM, it is believed to be less accurate, thus is not recommended for this particular method of determining nonlinearity.

With the addition of these two algorithms, the flowchart in Fig. 7.1 now contains all combinations of signal processing and signal tracking techniques. Those blocks which are crossed out represent the ineffective processes, while the best is highlighted in red.

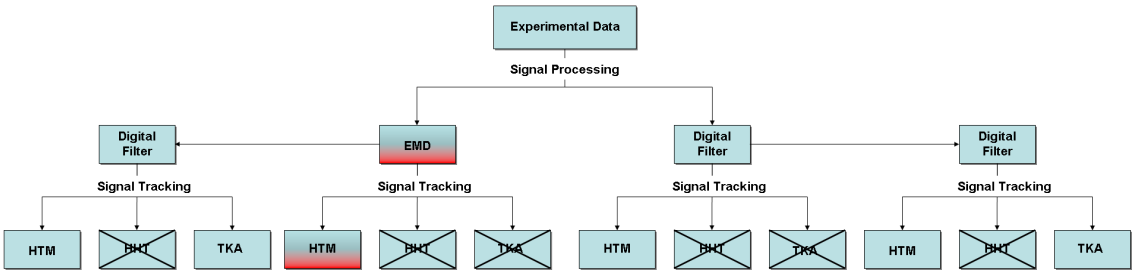

Figure 7.1. Flowchart with all effective algorithms

Analyzing and interpreting the results from the horizontal short beam experiment provide additional difficulties. The higher frequency and amplitude changes associated with the freely vibrating short cantilever beam decrease the resolution and effectiveness of all three signal tracking methods. More noise is introduced into the instantaneous frequency and amplitude calculations and plots are more spread out. Precisely determining the nonlinear coefficient also becomes more difficult as the least squares fit can become less accurate. However, this coefficient can still be seen to take a negative value. Additionally, by visually inspecting the amplitude versus frequency plots the relationship can clearly be characterized as softening; which also agrees with the other experimental results. Due to the level of accuracy within these calculations

and the results of the least-squares fit, few other comparisons can be made to the two other experiments with the longer beam.

Through this work it is shown how transient responses can be used to determine the nonlinear characteristics of a vibrating system. The Harmonics Tracking Method has proven to be a viable signal tracking technique for this type of analysis, and is shown to be superior to both the Teager-Kaiser Algorithm and the Hilbert-Huang Transform. Additionally, both signal processing techniques, when coupled with HTM, provide excellent data. Through further analysis, TKA has shown to also provide accurate data very similar to HTM with the use of an additional digital filter. Unfortunately, with the further use of the filter comes an additional phase shift and more distorted data must be ignored. For this reason it is suggested that for best results, the combination of EMD and HTM be used. Furthermore, HTM makes use of only three data points to calculate instantaneous frequency and amplitude; and does so accurately with less signal processing. With this, one can see how this technique can be used to perform these calculations simultaneously with incoming data for online signal tracking. This method does have some limitations. It can be seen how large and sudden fluctuations in signal frequency and amplitude can cause difficulties in precisely tracking an incoming signal, as is the case with the short cantilever beam. However, using transient vibration of structures has proven to be a viable method for determining nonlinearities of vibrating structures.

7.2 Recommendations for Future Work

It has been shown how transient analysis can be used for verifying nonlinear characteristics of the dynamic response of a system. This method makes use of both signal processing and signal tracking techniques. In order to demonstrate and test its viability it has been applied to three experiments involving a simple cantilever beam. Although within this work the motivation behind the research has been the dynamics of tuning fork MVGs, cantilever beams are used within numerous applications. It has also been proposed that for future applications of this method, HTM should be used in conjunction with EMD to yield the best results.

For future work, using transient analysis for determination of nonlinearity of more complex systems may be of interest. For example, analyzing the nonlinearities of a vibrating membrane, such as a drum or loudspeaker, may yield interesting results. Better predictions involving the response of the membrane of a speaker when attenuated may ultimately yield superior sound quality. Analyzing wave propagation through a medium is another experiment which may be performed with this type of analysis. Wind-generated nonlinear ocean waves are an area of specific interest within ocean engineering. A proximity sensor may be used to capture the transient response of a wave propagating. Instantaneous amplitude or frequency may then be found using this type of analysis and comparisons made to theory and other works such as that found in [8].

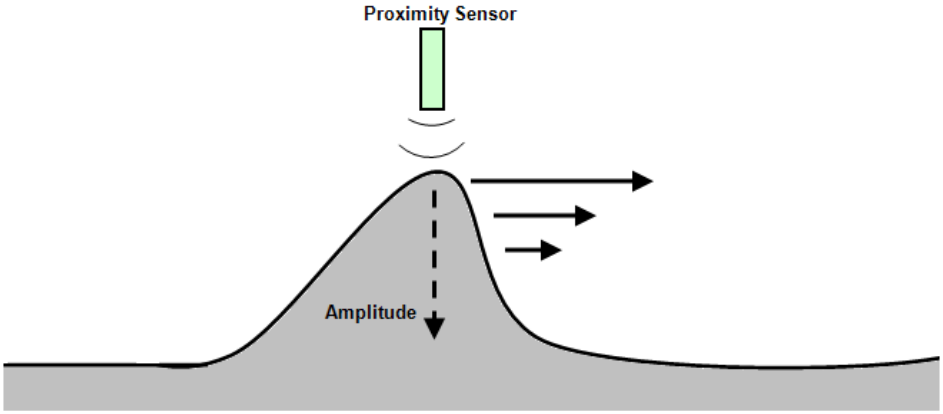

Figure 7.2. Sketch of wave propagation

There are many applications in which transient analysis of vibrating structures can be of use. The development of a nonlinear feedback control system could be expanded to the area of nonlinear vibration control. Being able to accurately calculate instantaneous amplitude and frequency response of a vibrating structure in real time is required for the feedback system to correctly control or dampen vibrations. This type of nonlinear vibration feedback controller may prove useful in the area of aerodynamics, where vibrations can be destructive to aircraft. In particular, certain conditions can result in a flapping like motion of a fixed wing aircraft which can lead to failure.

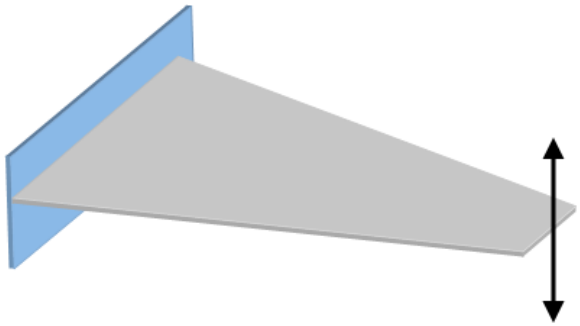

Figure 7.3. Sketch of aircraft wing experiencing "flapping" vibration

The use of transient vibrations as a method for determination of nonlinearity may also be used within the area of nondestructive evaluation. Monitoring or finding

structural damage is necessary in many applications of engineering. By analyzing a structure's transient response to a given input and comparing it to a known structurally sound system may help localize or determine the cause of damage.

Analyzing transient and non-stationary signals has proven in the past to be a very difficult area of study. However, recent advances in this area, namely the Hilbert-Huang transform, and the Harmonics Tracking Method, are making it feasible to achieve accurate results. This allows one to use transient vibrations as a method for determining the nonlinearity of vibrating structure, and hence has applications spanning a wide range of engineering. However, more research is needed to expand this method to more complex systems. Subsequently, comparisons can be drawn to numerical simulations and theoretical models for further validation.

REFERENCES

[1] Andrei M. Shkel, *Type I and Type II Micromachined Vibratory Gyroscopes*, pp. 586-593, IEEE/ION PLANS 2006, San Diego, CA, USA (invited)

[2] Acar, Cenk, and Andrei Shkel. *MEMS Vibratory Gyroscopes Strutural Approaches to Improve Robustness*. New York: Springer, 2009. Print.

[3] Lee, Yongsik. *A Study of Parametrically Excitation Applied to a MEMS Tuning Fork Gyroscope*. Thesis. University of Missouri - Columbia, 2007. Print.

[4] Hunang, Norden E. *Introduction to The Hilbert-Huang Transform and its Related Mathematical Problems*. Hilbert-Huang Transform and its Applications. Ed. Norden E. Huang & Samuel S P Shen. Hackensack: World Scientific Publishing Co. Pte. Ltd., 2005. 1-26.

[5] Huang, Norden E., Zheng Shen, Steven R. Long, Manli C. Wu, Hsing H. Shih, Quanan Zheng, Nai-Chyuan Yen, Chi Chao Tung, and Henry H. Liu. *The Empirical Mode Decomposition and the Hilbert Spectrum for Nonlinear and Non-Stationary Time Series Analysis*. Mathematical, Physical and Engineering Sciences 454 (1998): 903-95.

[6] P. Frank Pai, *Online tracking of instantaneous frequency and amplitude of dynamic system response*, Mechanical Systems and Signal Processing (2009), doi:10.1016/j.ymssp.2009.07.014

[7] Anderson, T. A., A. H. Nayfea, and B. Balachandran. "Experimental Verification of the Importance of the Nonlinear Curvature in the Response of a Cantilever Beam." Journal of Vibration and Acoustics 118 (1996): 21-27.

[8] Hwang, Paul A., Norden E. Huang, David W. Wang, and James M. Kaihatu. *Hilbert Spectra of Nonlinear Ocean Waves*. Hilbert-Huang Transform and its Applications. Ed. Norden E. Huang & Samuel S P Shen. Hackensack: World Scientific Publishing Co. Pte. Ltd., 2005. 1-26.

[9] Lee, Yongsik, P. Frank Pai, and Z. C. Feng. *Nonlinear Complex Response of a Parametrically Excited Tuning Fork*. Mechanical Systems and Signal Processing 22 (2007): 1146-156.

[10] Vakman, David. *On the Analytical Signal, the Teager-Kaiser Energy Algorithm, and Other Methods for Defining Amplitude and Frequency.* IEEE Transactions on Signal Processing 44 (1996): 791-97.

[11] Boulter, Brian T. *Digital Filter Design Writing Difference Equations for Digital Filters.* ApICS. 2000. ApICS. 27 May 2008 <http:/www.apicsllc.com>.

[12] Nayfeh, Ali Hasan, and Dean T. Mook. *Nonlinear Oscillations*. New York: Wiley,1979. Print.

[13] Virgin, Lawrance N. *Vibration of Axially Loaded Structures*. New York: Cambridge UP, 2007. Print.

[14] Norden, Huang E., and Shen S P Samuel. *Hilbert-Huang Transform and its Applications*. Vol. 5. Hackensack: World Scientific Co. Pte. Ltd., 2005. Print.

Appendix A.1
MatLab Program for 4th Order Low Pass Digital Filter Examples

A.1.1 Example – Filtering the sum of two pure signals

```
%%%%%%%%%%%%%%%%%%%%%%%%%%%%%%%%%%%%%%%%%%%%%%%%%%%%
%                  Joe Dinardo                      %
%                                                   %
%            University of Missouri                 %
%                                                   %
%    4th Order Low-pass Digital Filter              %
%                                                   %
%      Example - Filtering the sum                  %
%                of two pure signals                %
%%%%%%%%%%%%%%%%%%%%%%%%%%%%%%%%%%%%%%%%%%%%%%%%%%%%


clc;clear;

close all

%Defining variables
T=.00025;  % Sampling Rate
t=0:T:8;   % Creating time matrix
a1=5;      % Amplitude of y1
a2=2;      % Amplitude of y2
f1=8;      % Frequency of y1
f2=50;     % Frequency of y2

%Defining y1
y1=a1*cos(2*pi*f1*t);
subplot(3,1,1)
plot(t,y1,'k')
title('y_1 vs. Time')
xlabel('Time [s]');ylabel('y_1')
axis([0 1 -a1 a1]); grid on


%Defining y2
y2=a2*cos(2*pi*f2*t);
subplot(3,1,2)
plot(t,y2,'k')
title('y_2 vs. Time')
xlabel('Time [s]');ylabel('y_2')
axis([0 1 -a2 a2]); grid on

%Defining Y
subplot(3,1,3)
Y=y1+y2;
plot(t,Y,'k');axis([0,2,-7,7]); grid on
title('Y=y_1+y_2 vs. Time')
xlabel('Time [s]'); ylabel('Y')


%%%%%%%%%%%%%%%%%%%%%%% DIGITAL FILTER DESIGN %%%%%%%%%%%%%%%%%%%%%%%%%

%% 4th Order Low Pass Filter %%

% Setting parameters for digital filter
```

```
x = Y;
time = t;

freq0 = f1+.4*f1;  % Setting cut off frequency for D-Filter - Use to filter out y1


wd=freq0;
c=cot(2*pi*wd*T/2);


%Defining "n" coefficients

n0=1;

n1=4;

n2=6;

n3=4;

n4=1;



%Defining "d" coefficients

d0=(1+c^2+(3*sqrt(26)/20)*c)*(1+c^2+(181*sqrt(26)/500)*c);

d1=(4/125)*(1-c^2)*(125*(1+c^2)+32*sqrt(26)*c);

d2=(1/5000)*(30000*(1+c^4)-34118*c^2);

d3=(4/125)*(1-c^2)*(125*(1+c^2)-32*sqrt(26)*c);

d4=(1+c^2-(3*sqrt(26)/20)*c)*(1+c^2-(181*sqrt(26)/500)*c);

x=x(end:-1:1);   % Reversing the order of elements to back-feed filter

F=[x(1) x(2) x(3) x(4)];

% Filtering Data
for i=5:length(x)

     F(i)=((n0*x(i)+n1*x(i-1)+n2*x(i-2)+n3*x(i-3)+n4*x(i-4))+(-d1*F(i-1)-d2*F(i-2)-
d3*F(i-3)-d4*F(i-4)))/d0;

end

% Plotting the incoming signal and filtered incoming signal

time=time(end:-1:1);   % Reverse the order of elements again to plot forward
figure(3)
subplot(2,1,1);plot(time,x,'k');xlabel('Time [s]');ylabel('Incoming Signal
[Y]');axis([0,9,-10,10]); grid on
title('4^t^h Order Low Pass Digital Filtering');
subplot(2,1,2);plot(time,F,'g');xlabel('Time [s]');ylabel('Filtered Incoming
Signal');axis([0,9,-40,20]); grid on


% Redefining axes and plotting incoming signal, filtered incoming signal, and original y1
signal
figure(4)
subplot(3,1,1);plot(time,x,'k');xlabel('Time [s]');ylabel('Incoming Signal
[Y]');axis([0,2,-7,7]); grid on
title('4^t^h Order Low Pass Digital Filtering');
subplot(3,1,2);plot(time,F,'g');xlabel('Time [s]');ylabel('Filtered Incoming
Signal');axis([0,2,-7,7]); grid on
subplot(3,1,3);plot(time,y1,'k');xlabel('Time [s]');ylabel('Original Signal
[y_1]');axis([0,2,-7,7]); grid on
```

A.1.2 Example – Filtering White Noise From One Pure Signal

```
%%%%%%%%%%%%%%%%%%%%%%%%%%%%%%%%%%%%%%%%%%%%%
%                 Joe Dinardo               %
%                                           %
%            University of Missouri         %
%                                           %
%   4th Order Low-pass  Digital Filter      %
%                                           %
%     Example - Filtering white noise       %
%               from one pure signal        %
%%%%%%%%%%%%%%%%%%%%%%%%%%%%%%%%%%%%%%%%%%%%%


clc;clear;

close all

%Defining variables
T=.00025;  % Sampling Rate
t=0:T:8;   % Creating time matrix
a1=5;       % Amplitude of y1
f1=8;       % Frequency of y1


%Defining y1
y1=a1*cos(2*pi*f1*t);

%Defining Y
for i=1:length(t)
Y(i)=a1*cos(2*pi*f1*t(i))+1.5*unifrd(-1,1);
end


figure(1)
subplot(2,1,1)
plot(t,y1,'k')
axis([0 1 -8 8])
title('y_1 vs. Time');grid on
xlabel('Time [s]')


subplot(2,1,2)
plot(t,Y,'k')
axis([0 1 -8 8])
title('Y=y_1+White Noise vs. Time')
xlabel('Time [s]');grid on

% subplot(3,1,3)
% plot(t,Y)
% axis([0 .2 -8 8])
% title('Y=y_1+White Noise vs. Time')
% xlabel('Time [s]');grid on


%%%%%%%%%%%%%%%%%%%%%% DIGITAL FILTER DESIGN %%%%%%%%%%%%%%%%%%%%%%%%%

%% 4th Order Low Pass Filter %%

% Setting parameters for digital filter
x = Y;
time = t;

freq0 = f1+.4*f1;  % Setting cut off frequency for D-Filter - Use to filter out y1
```

```
wd=freq0;
c=cot(2*pi*wd*T/2);


%Defining "n" coefficients

n0=1;

n1=4;

n2=6;

n3=4;

n4=1;



%Defining "d" coefficients

d0=(1+c^2+(3*sqrt(26)/20)*c)*(1+c^2+(181*sqrt(26)/500)*c);

d1=(4/125)*(1-c^2)*(125*(1+c^2)+32*sqrt(26)*c);

d2=(1/5000)*(30000*(1+c^4)-34118*c^2);

d3=(4/125)*(1-c^2)*(125*(1+c^2)-32*sqrt(26)*c);

d4=(1+c^2-(3*sqrt(26)/20)*c)*(1+c^2-(181*sqrt(26)/500)*c);

x=x(end:-1:1);   % Reversing the order of elements to back-feed filter

F=[x(1) x(2) x(3) x(4)];

% Filtering Data
for i=5:length(x)

     F(i)=((n0*x(i)+n1*x(i-1)+n2*x(i-2)+n3*x(i-3)+n4*x(i-4))+(-d1*F(i-1)-d2*F(i-2)-
d3*F(i-3)-d4*F(i-4)))/d0;

end

% Plotting the incoming signal and filtered incoming signal

time=time(end:-1:1);   % Reverse the order of elements again to plot forward
figure(3)
subplot(2,1,1);plot(time,x,'k');xlabel('Time [s]');ylabel('Incoming Signal
[Y]');axis([0,9,-10,10]); grid on
title('4^t^h Order Low Pass Digital Filtering');
subplot(2,1,2);plot(time,F,'g');xlabel('Time [s]');ylabel('Filtered Incoming
Signal');axis([0,9,-40,20]); grid on



% Redefining axes and plotting incoming signal, filtered incoming signal, and original y1
signal
figure(4)
subplot(3,1,1);plot(time,x,'k');xlabel('Time [s]');ylabel('Incoming Signal
[Y]');axis([0,2,-7,7]); grid on
title('4^t^h Order Low Pass Digital Filtering');
subplot(3,1,2);plot(time,F,'g');xlabel('Time [s]');ylabel('Filtered Incoming
Signal');axis([0,2,-7,7]); grid on
subplot(3,1,3);plot(time,y1,'k');xlabel('Time [s]');ylabel('Original Signal
[y_1]');axis([0,2,-7,7]); grid on
```

Appendix A.2
MatLab Program for Simulation of Nonlinear Damped Pendulum

A.2.1 Pendulum Simulation Main Program

```
%% Program Simulates a Damped/Forced(OPTIONAL) Pendulum Swinging %%

clc;clear;close all

global g L m gamma A omega

% Can change the parameters below
%%%%%%%%%%%%%%%%%%%%%%%%%%%%%%%%%%%%%%%%%%%%%%%%%%%%%%%%%%%%%%%%%%%%%%%%%%%%%%%
L = .1;  % Length of string [m]
m = 5;  % Mass of pendulum [kg]
g = 9.81; % Gravity  [m/s^2]
gamma = .3;  % Dampening ratio
TSim = 50; % Total time of simulation [s]
Theta0 = 135;  % Starting position for pendulum [deg]
Theta_dot0 = 0; % Initial angular velocity of pendulum
A = 0; % Forcing Amplitude [N]
omega = 0;  % Forcing freqency
%%%%%%%%%%%%%%%%%%%%%%%%%%%%%%%%%%%%%%%%%%%%%%%%%%%%%%%%%%%%%%%%%%%%%%%%%%%%%%%


%% For More Accuracy
%%%%%%%%%%%%%%%%%%%%%%%%%%%%%%%%%%%%%%%%%%%%%%%%%%%%%%%%%%%%%%%%%%%%%%%%%%%%%%%
y0 = [Theta0 Theta_dot0];  %Initial Conditions for ode solver
tstep=.005;  % Time step for ode solver
totalsteps=TSim/tstep;




% Running ode solver while controlling time step

for z=1:totalsteps

    tspan=[(z-1)*tstep z*tstep];

    [Time Data]=ode113('PendSub',tspan,y0);

    y0=Data(end,1:end);

    if z == 1
    Sol = Data(end,1:end);
    Sol_Time = Time(end,1:end);
    else
    Sol=cat(1,Sol,Data(end,1:end));
    Sol_Time = cat(1,Sol_Time,Time(end,1:end));
    end

end


% Outputting Solution From ode solver
Theta = Sol(:,1);
Theta_dot = Sol(:,2);
```

```
Time = Sol_Time;


%  Plotting Thets vs. Time
figure(1)
hold on
grid on
title('Theta vs. Time'); xlabel('Time [s]'); ylabel('Theta [deg]')
plot(Time, Theta)
 %Outputting Theta vs Time Data to .txt file
out=[Time, Theta];  save Pendulum.txt out  -ascii


%  Plotting Theta dot vs. Time
figure(2)
hold on
grid on
title('Theta dot  vs. Time'); xlabel('Time [s]'); ylabel('Theta dot [deg/s]')
plot(Time, Theta_dot)


%  Plotting the Phase Plane Diagram
figure(3)
hold on
grid on
title('Pendulum Phase Plane');xlabel('Theta [deg]'); ylabel('Theta dot [deg/s]')
plot(Theta,Theta_dot)


%Calculating Pendulum Positions
Theta_2=Theta(1:20:length(Theta),:); %down sampling if a high sampling frequency is used
%-->MODIFY HERE
x=L*sind(Theta_2);
y=-L*cosd(Theta_2);


%  Plotting Simulation and saving MatLab Movie
figure(4)

for i = 1:length(x)
    plot(0,0,'s','MarkerSize',12,'MarkerFaceColor','r');axis([-(L+.25*L) (L+.25*L) -
(L+.25*L) (L+.25*L)])
    grid on; hold on
    plot(x(i),y(i),'bo','MarkerSize',12,'MarkerFaceColor','b');
    line([0,x(i)],[0,y(i)]);
    F(i)=getframe;
    hold off

end


%  Plotting Figure Which Shows Pendulum at Multiple Positions
figure(5)
hold on
grid on
title('Pendulum Simulation')
pic=[1 80 87 100 110 120];
for i = 1:length(pic)
plot(0,0,'s','MarkerSize',12,'MarkerFaceColor','r');axis([-(L+.25*L) (L+.25*L) -(L+.25*L)
(L+.25*L)])
    plot(x(pic(i)),y(pic(i)),'bo','MarkerSize',12,'MarkerFaceColor','b');
    line([0,x(pic(i))],[0,y(pic(i))]);
end
```

A.2.2 Pendulum Simulation Sub Program

```
% Pendulum Simulation Sub Program


function ydot = PendSub(time,y0)

global g L m gamma A omega

% y0 is a vector where the first element is Theta and the second
% element is Theta_dot

% Damped / Forced(OPTIONAL) Pendulum

Td = y0(2);  % Theta dot
Tdd = -(g/L)*sind(y0(1))-gamma/m*Td+A*sind(omega*time);  %Theta double dot ( Equation of
motion)


%Creating vector for ode solver
ydot = [Td Tdd]';
```

Appendix A.3

MatLab Program for Teager-Kaiser Data Processing / Digital Filter

A.3.1 Main MatLab Program for Teager-Kaiser Algorithm / Digital Filtering

```
%%%          Joe Dinardo            %%%
%       University of Missouri       %
%  Main  Signal Processing File      %
%  which will use Low Pass Filter    %
%          and TK Method             %
%%%%%%%%%%%%%%%%%%%%%%%%%%%%%%%%%%%%

clc;clear;close all
%Loading Data
load Feb19_2009_4.txt
XX=Feb19_2009_4;

nfft=size(XX,1);
XX=XX(1:1:nfft,:); %down sampling if a high sampling frequency is used
x=XX(:,2);  %Incoming Signal Data
time=XX(:,1); % Time Data
dt=[time(nfft,1)-time(1,1)]/(nfft-1);  %Delta t of time vector


% Plotting Freqency Spectrum of Incoming Signal
Y=fft(x); % FFT spectrum, for reference purpose
nfft2=nfft/2; nfft21=nfft2+1;
th=[1; 2*ones(nfft2-1,1); 1]/nfft;
a=real(Y(1:nfft21)).*th; b=-imag(Y(1:nfft21)).*th;
fre=[0:nfft2]/(time(nfft)+dt); mag=(a.^2+b.^2).^0.5;
figure(1)
G=plot(fre,20*log10(mag),char('r')); set(G,'linewidth',0.9), xlabel(sprintf('frequency
(Hz)')),  ylabel('10log_{10}(PSD)')
title('Frequency Domain of Incoming Signal')
grid on
clear Y nfft2 nfft21 th a b fre mag G

%%%  Low Pass Filtering  %%%
%Setting parameters
freq0=50;  %Frequency for Low Pass Filter

T=dt;
%Calling Low Pass Filter
F=Lowpass(x,time,freq0,T);


% Plotting Freqency Spectrum of Filtered Signal
Y=fft(F); % FFT spectrum, for reference purpose
nfft2=nfft/2; nfft21=nfft2+1;
th=[1; 2*ones(nfft2-1,1); 1]/nfft;
a=real(Y(1:nfft21))'.*th; b=-imag(Y(1:nfft21))'.*th;
fre=[0:nfft2]/(time(nfft)+dt); mag=(a.^2+b.^2).^0.5;
figure(2)
P=plot(fre,20*log10(mag),char('r')); set(P,'linewidth',0.9), xlabel(sprintf('frequency
(Hz)')),  ylabel('10log_{10}(PSD)')
title('Frequency Domain of Filtered Signal')
grid on


%%% Using TK on Filtered Data %%%
```

```
[a freq]=TK(F,T,time);

% All results in one plot
time=time(end:-1:1);    % Reverse the order of elements because of "back feeding of data"
figure(5)
subplot(2,2,1);plot(time,F);xlabel('Time [s]');ylabel('Filtered Incoming
Signal');axis([0,5,-1,1]); grid on
subplot(2,2,2);plot(fre,20*log10(mag),char('r')); set(P,'linewidth',0.9),
xlabel(sprintf('frequency (Hz)')),  ylabel('10log_{10}(PSD)');grid on
subplot(2,2,3);plot(time,a);xlabel('Time [s]');ylabel('Amplitude');axis([0,10,0,1]);grid
on
subplot(2,2,4);plot(time,freq);xlabel('Time [s]');ylabel('Frequency
[Hz]');axis([0,5,3.8,3.95]);grid on

ax = axes('position',[0,0,1,1],'visible','off');
tx = text(0.3,.975,'TK results from short beam after digital filter');
set(tx,'fontweight','bold');


%Ploting Frequency vs amplitude
figure(6)
plot(freq,a);xlabel('Frequency [Hz]');ylabel('Amplitude [m/s]');grid on
figure(7)
plot(a,freq);ylabel('Frequency [Hz]');xlabel('Amplitude [m/s]');grid on
```

A.3.2 MatLab Sub Program for Digital Filtering

```
%% Subprogram for 4th order Low Pass Digital Filter %%
%% Low Pass Filter Design %%

function F=lowpass(x,time,freq0,T)
%%%%%%%%%%%%%%%%%%%%%% DIGITAL FILTER DESIGN %%%%%%%%%%%%%%%%%%%%%%%%%

%% 4th Order Low Pass Filter %%

wd=freq0;
c=cot(2*pi*wd*T/2);


%Defining "n" coefficients

n0=1;

n1=4;

n2=6;

n3=4;

n4=1;



%Defining "d" coefficients

d0=(1+c^2+(3*sqrt(26)/20)*c)*(1+c^2+(181*sqrt(26)/500)*c);

d1=(4/125)*(1-c^2)*(125*(1+c^2)+32*sqrt(26)*c);

d2=(1/5000)*(30000*(1+c^4)-34118*c^2);

d3=(4/125)*(1-c^2)*(125*(1+c^2)-32*sqrt(26)*c);

d4=(1+c^2-(3*sqrt(26)/20)*c)*(1+c^2-(181*sqrt(26)/500)*c);
```

```
x=x(end:-1:1);   % Reversing the order of elements to back-feed filter
F=[x(1) x(2) x(3) x(4)];

% Filtering Data
for i=5:length(x)

     F(i)=((n0*x(i)+n1*x(i-1)+n2*x(i-2)+n3*x(i-3)+n4*x(i-4))+(-d1*F(i-1)-d2*F(i-2)-
d3*F(i-3)-d4*F(i-4)))/d0;

end


time=time(end:-1:1);   % Reverse the order of elements
figure(3)
subplot(2,1,1);plot(time,x);xlabel('Time [s]');ylabel('Incoming Signal');axis([0,10,-
.8,.8]); grid on
title('Low Pass Filtering');
subplot(2,1,2);plot(time,F);xlabel('Time [s]');ylabel('Filtered Incoming
Signal');axis([0,11,-.8,.8]); grid on
```

A.3.3 MatLab Sub Program for Taeger-Kaiser Algorithm

```
%%% Subprogram for Teager-Kaiser Algorithm %%%

%% Implementing Teager-Kaiser Algorithm on incoming signal %%


function [a freq]=TK(F,T,time)
for i=5:length(F)

        u(i)=(-F(i-3)+9*F(i-2)+9*F(i-1)-F(i))/16;
        up(i)=(F(i-3)-27*F(i-2)+27*F(i-1)-F(i))/(24*T);
        upp(i)=(F(i-3)-F(i-2)-F(i-1)+F(i))/(2*T^2);
        uppp(i)=(-F(i-3)+3*F(i-2)-3*F(i-1)+F(i))/(T^3);
        Psi_u(i)=up(i)^2-u(i)*upp(i);
        Psi_up(i)=upp(i)^2-up(i)*uppp(i);
        a(i)=Psi_u(i)/sqrt(Psi_up(i));
        freq(i)=sqrt(Psi_up(i)/Psi_u(i))/(2*pi);

end

time=time(end:-1:1);   % Reverse the order of elements

% Plotting
figure(4)
title('Mode 1 anlysis from Data din2.txt');
subplot(3,1,1);plot(time,F);xlabel('Time [s]');ylabel('Filtered Incoming Signal');grid on
subplot(3,1,2);plot(time,a);xlabel('Time [s]');ylabel('Amplitude');grid on
subplot(3,1,3);plot(time,freq);xlabel('Time [s]');ylabel('Frequency [Hz]');grid on
```

Appendix A.4
MatLab Program for Empirical Mode Decomposition

A.4.1 MatLab Initial Program for EMD Analysis

```
%%%%%%%%%%%%%%%%%%%%%%%%%%%%%%%%%%%%%%%%%%%%%%%%%%%%
%                  Joe Dinardo                      %
%                                                   %
%            University of Missouri                 %
%                                                   %
%          Empirical Mode Decomposition             %
%                                                   %
%      Example - Decomposing the sum                %
%                of two pure signals                %
%             This program calls emd.m              %
%%%%%%%%%%%%%%%%%%%%%%%%%%%%%%%%%%%%%%%%%%%%%%%%%%%%


clc;clear;

close all

%Defining variables
T=.001;  % Sampling Rate
t=0:T:8;   % Creating time matrix
a1=5;      % Amplitude of y1
a2=2;      % Amplitude of y2
f1=8;      % Frequency of y1
f2=50;     % Frequency of y2

%Defining y1
y1=a1*cos(2*pi*f1*t);
subplot(3,1,1)
plot(t,y1,'k')
title('y_1 vs. Time')
xlabel('Time [s]');ylabel('y_1')
axis([0 1 -a1 a1]); grid on


%Defining y2
y2=a2*cos(2*pi*f2*t);
subplot(3,1,2)
plot(t,y2,'k')
title('y_2 vs. Time')
xlabel('Time [s]');ylabel('y_2')
axis([0 1 -a2 a2]); grid on


%Defining Y
subplot(3,1,3)
Y=y1+y2;
plot(t,Y,'k');axis([0,2,-7,7]); grid on
title('Y=y_1+y_2 vs. Time')
xlabel('Time [s]'); ylabel('Y')


Yt =cat(2,t',Y');
```

```
%Outputting Y vs Time Data to .txt file
out=[t', Y'];  save Yt.txt out  -ascii


time=t';

% Calling Empirical Mode Decomposition to Extract IMFs
imf = emd(Y',time);


%Plotting
plots = size(imf);

    figure(30)
    subplot(plots(1)+1,1,1);plot(t',Y); grid on;hold on;title('EMD
Analysis');ylabel('Y');axis([0 1 -8 8]);

    for i = 1:plots(1)

      subplot(plots(1)+1,1,i+1); plot(t,imf(i,:));grid
on;ylabel(['c_',num2str(i)]);axis([0 1 -8 8]);
    end
```

A.4.2 MatLab Main Program for EMD Analysis

```
%%%%%%%%%%%%%%%%%%%%%%%%%%%%%%%%%%%%%%%%%%%%%%%%%%%%
%                 Joe Dinardo                 %
%                                             %
%           University of Missouri            %
%                                             %
%         Empirical Mode Decomposition        %
%                                             %
%     Example - Decomposing the sum           %
%               of two pure signals           %
%                 MAIN EMD PROGRAM            %
%%%%%%%%%%%%%%%%%%%%%%%%%%%%%%%%%%%%%%%%%%%%%%%%%%%%
% This program will result in slight edge effects within the extracted IMFs %


% Call function as:
% imf = emd(Y,time)
%
% Defining x and n
% Y = Input signal (column vector)
% n = Number of IMFs to be extracted from Y



function imf = emd(Y,time);

%Calling user to input the number of IMFs to be isolated
n = input('Enter The Number of IMFs To Be Isolated From The Incoming Signal:  ')

x0 = Y(:)'; % Copying the input signal,x and turning intoa a row vector
N = length(Y);
counter = 0;  % Initializing Counter for Loop

%==== Starting EMD Loop ====%
%=================================================================%
% loop to decompose the input signal into n successive IMFs

imf = []; % Initializing Matrix which contains all isolated IMFs

for t=1:n % loop on successive IMFs
```

```
   %-------------------------------------------------------------------------
   % inner loop to find each imf

   h = x0; % at the beginning of the sifting process, h is the signal
   SD = 1; % Initializing Standard deviation to start sifting process

   while SD > 0.1 % while the standard deviation is higher than 0.1
      counter = counter+1; % Adding to loop counter

      % Finding local extrema by finding zeros of derivative
      d = diff(h); % MatLab's derivative Command
      max_min = []; % Initializing matrix which will store local extrema
      for i=1:N-2
         if d(i)==0      % Checking to find Zeros of derivative
           if sign(d(i-1))~=sign(d(i+1))  % Then maximum is found
               max_min = [max_min, i];
            end
         elseif sign(d(i))~=sign(d(i+1))
            max_min = [max_min, i+1];
         end
      end

      if size(max_min,2) < 2 % If number of max or min in less than two only residue is
left and IMFs have been extracted
         break
      end

      % Dividing matrix max_min into local maxima and minima
      if max_min(1)>max_min(2)   %--> Finding if first point is a max or min
         maxes = max_min(1:2:length(max_min));
         mins  = max_min(2:2:length(max_min));
      else
         maxes = max_min(2:2:length(max_min));
         mins  = max_min(1:2:length(max_min));
      end

      % Making endpoints both maxes and mins  (Will Alter Edge Effects)
      maxes = [1 maxes N];  % For example used in EMD_Ex.m this is best when extracting
first IMF
      %mins  = [1 mins  N];


      %=========================================================================
      % Calling Cubic Spline for determining max and min envelopes        %
      %=========================================================================

      maxenv = spline(maxes,h(maxes),1:N);
      minenv = spline(mins, h(mins),1:N);

      m = (maxenv + minenv)/2; %--> Finding the average of the two envelopes


      prevh = h; % Defining previous value of h before subtracting the mean from it (to
be used within SD calculations)
      h = h - m; % Subtracting the mean of the two envelopes from h to continue sifting
process


      %  Plotting the Results of the First Sifting Process in Two Figures
      if counter == 1;
     figure(2);
     subplot(3,1,1);plot(time,Y,'LineWidth',1);axis([0 .5 -8 8]);grid on;title('Incoming
signal, Y');xlabel('Time [s]');
     subplot(3,1,2);hold on;plot(time,Y,'LineWidth',1);plot(time,maxenv,'r');axis([0 .5 -
8 8]);title('Y and Maxima Envelope');grid on
     subplot(3,1,3);hold on;plot(time,Y,'LineWidth',1);plot(time,minenv,'m');axis([0 .5 -
8 8]);title('Y and Minima Envelope');grid on

     figure(3);
     subplot(2,1,1);hold on; plot(time,Y,'LineWidth',2);plot(time,maxenv,'r');
     plot(time,minenv,'m');plot(time,m,'k','LineWidth',2);
```

```
     axis([0 .5 -8 8]); grid on; title('EMD Analysis'); xlabel('Time [s]');
legend('Incoming signal, Y','Maxima Envelope','Minima Envelope','Envelope Mean, m_1')
     subplot(2,1,2);hold on; plot(time,h);axis([0 .5 -2 2]);xlabel('Time
[s]');legend('h_1'); grid on

      end

      % Calculating SD for criteria to stop sifting loop
      alpha = 0.00000001; % To Avoid division by zero error
      SD = sum ( ((prevh - h).^2) ./ (prevh.^2 + alpha) );

   end

   % Saving the extracting IMFs in a single matrix
   imf = [imf; h];


   % Stopping Loop if only residue is left
   if size(max_min,2) < 2
      break
   end

   x0 = x0 - h; % Subtracting the isolated IMF form the original incoming signal

end
```